

AFIT/GEE/ENV/95D-16

A COMPARISON OF RESPONSE SURFACE
METHODOLOGY AND A ONE-FACTOR-AT-A-TIME
APPROACH AS CALIBRATION TECHNIQUES
FOR THE BIOPLUME-II SIMULATION
MODEL OF CONTAMINANT
BIODEGRADATION

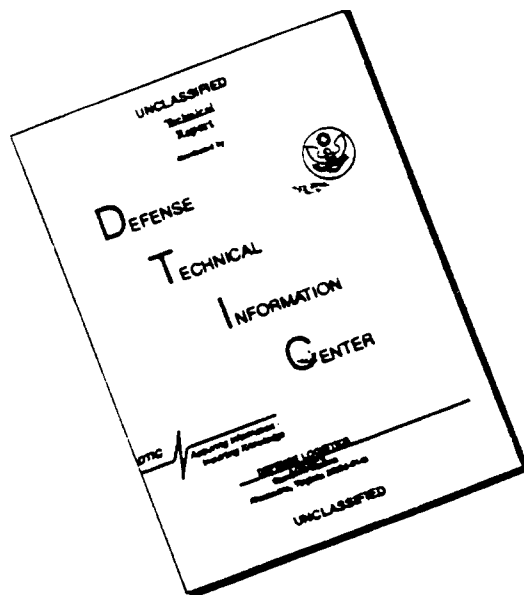
THESIS
Benjamin Shuman

AFIT/GEE/ENV/95D-16

Approved for public release; distribution unlimited

19960328 065

DISCLAIMER NOTICE



THIS DOCUMENT IS BEST
QUALITY AVAILABLE. THE COPY
FURNISHED TO DTIC CONTAINED
A SIGNIFICANT NUMBER OF
PAGES WHICH DO NOT
REPRODUCE LEGIBLY.

The views expressed in this thesis are those of the author and do not reflect the official policy or position of the Department of Defense or the U. S. Government.

A COMPARISON OF RESPONSE SURFACE METHODOLOGY AND A
ONE-FACTOR-AT-A-TIME APPROACH AS CALIBRATION
TECHNIQUES FOR THE BIOPLUME-II SIMULATION MODEL OF
CONTAMINANT BIODEGRADATION

THESIS

Presented to the Faculty of the School of Engineering
of the Air Force Institute of Technology
Air University
In Partial Fulfillment of the
Requirements for the Degree of
Master of Science in Engineering and Environmental Management

Benjamin Shuman

December 1995

Approved for public release; distribution unlimited

A COMPARISON OF RESPONSE SURFACE METHODOLOGY AND A
ONE-FACTOR-AT-A-TIME APPROACH AS CALIBRATION TECHNIQUES FOR THE
BIOPLUME-II SIMULATION MODEL OF CONTAMINANT BIODEGRADATION

THESIS

Benjamin Shuman

Presented to the Faculty of the School of Engineering
of the Air Force Institute of Technology
Air University
In Partial Fulfillment of the
Requirements for the Degree of
Master of Science in Engineering and Environmental Management

Paul F. Auclair, Lt Col, USAF
Head, Department of
Operational Sciences

David L. Coulliette, Lt Col (sel), USAF
Assistant Professor, Department of
Mathematics and Statistics

Charles A. Bleckmann, PhD
Assistant Professor, Department of
Engineering and Environmental Management

Acknowledgements

I would like to thank my thesis committee: Lt Col Auclair, Lt Col (sel) Coulliette and Dr. Bleckman for their many hours of advice and assistance. Maj Heyse, Professor Dan Reynolds and Lt Col Hartley were each very helpful in answering questions. I would also like to thank Dr. Stauffer for providing me with the data related to the MADE-2 site and Dr. Rifai of Rice University for taking the time to answer my questions related to Bioplume II and providing me with the Unix source code. Captains Dave Schuchardt and Rob Sackett also deserve thanks for showing me the \LaTeX way. Thanks also to my wife Lori for her patience and to my children Aaron and Emilia for just being there. Finally, thanks to the Lord for giving me the ability to complete this work.

Benjamin Shuman

Table of Contents

	Page
Acknowledgements	iii
List of Figures	vii
List of Tables	viii
Abstract	x
I. Introduction	1
1.1 Motivation for Research	1
1.2 Research Objectives	2
II. Literature Review: The Inverse Problem	3
2.1 Trial and Error	4
2.2 Direct Methods	4
2.3 Indirect Methods	5
2.4 Geostatistical Approach	6
2.5 Sensitivity Analysis	7
2.6 Parameterization	8
2.7 Summary	9
III. Background	10
3.1 Bioplume II	10
3.2 Calibration Techniques	10
3.2.1 One Factor at a Time Calibration	11
3.2.2 Response Surface Methodology	12

	Page
IV. Experimentation	15
4.1 Description	15
4.1.1 Mathematical Setting of the Problem	16
4.2 Conduct	16
4.2.1 Input File Preparation	17
4.2.2 Final Condition	22
4.2.3 One-Factor-at-a-Time Approach	22
4.2.4 RSM Approach	31
4.3 Summary	43
V. Conclusions and Recommendations	45
5.1 Conclusions	45
5.2 Recommendations	47
Appendix A. Biodegradation of Petroleum Hydrocarbons	48
Appendix B. Initial Bioplume Input File	58
Appendix C. SAS Output	60
C.1 Stepwise Procedure for RSM Screening Phase	60
C.2 First Run of the First-Order Design Phase	62
C.3 40% Design without Centerpoint	64
C.4 40% Design With Centerpoint	65
C.5 5% Design Around 50% Step along Gradient	66
C.6 5% Design on Step 9 Point	68
C.7 First Ridge Analysis	69
C.8 Screening Design for Transport Calibration	73
C.9 First-Order Design for RSM Transport Calibration	75
C.10 Ridge Analysis for RSM Transport Calibration	76

	Page
Appendix D. FORTRAN	82
D.1 Root Mean Squared Error Criterion Program	82
Bibliography	85
Vita	90

List of Figures

Figure	Page
1. RMS Error vs. Diffuse Discharge Rate	26
2. RMS Error vs. Transmissivity	27
3. RMS Error vs. Discharge	28
4. Graph of RMS Flow Along Gradient Vector	36
5. Graph of RMS Flow Along Second Gradient Vector	39
6. Biodegradation of Benzene to Catechol	53
7. Ortho-Cleavage Pathway	54
8. Meta-Cleavage Pathway	55
9. Anaerobic, Ring Hydroxylation of Benzene	56
10. Anaerobic, Methyl-Oxidation of Toluene	57

List of Tables

Table		Page
1.	Values of Transmissivity and RMS Error	23
2.	Values of Porosity and RMS Error Criteria	24
3.	Diffuse Recharge and Required Particle Moves	25
4.	Diffuse Discharge and RMS Error Criteria	25
5.	Recalibration on Transmissivity	26
6.	Recalibration on Porosity	27
7.	Recalibration on Discharge	28
8.	Values of Longitudinal Dispersivity and RMS Error	29
9.	Ratio of Longitudinal to Transverse Dispersivity and RMS Error	29
10.	Stoichiometric Ratio and RMS Error	30
11.	Distribution Coefficient and RMS Error	31
12.	Reaeration coefficient and RMS Error	31
13.	Levels of Flow Parameters	32
14.	Screening Design and RMS Error	33
15.	First Run of the First-Order Design Phase and RMS Error	33
16.	Second Run of the First-Order Design Phase and RMS Error	34
17.	Centerpoint of Previous Design and RMS Error	34
18.	Table of Calculations for Steepest Descent Gradient	35
19.	Table of RMS Flow Values along First Gradient Vector	36
20.	Run of a 5% Design Centered on 5th Step	37
21.	Table of Calculations for Second Steepest Descent Gradient	37
22.	Table of RMS Flow Values along Second Gradient Vector	38
23.	Run of a 5% Design Centered on 9th Step	38
24.	Additional Points Centered on 9th Step	38
25.	Ridge Analysis for RSM Flow Calibration	40

Table	Page
26. Details of Screening Design Levels	41
27. First-Order Design for RSM Transport Calibration	42
28. Second-Order Design for RSM Transport Calibration	42
29. Ridge Analysis for RSM Transport Calibration	43
30. Summary of Calibrations	43

Abstract

This thesis compared the Response Surface Methodology (RSM) approach to the one-factor-at-a-time approach for calibrating the Bioplume II finite-difference simulation model of groundwater flow, contaminant transport and biodegradation. The MADE-2 data set of hydrocarbon injection into pristine groundwater at Columbus Air Force Base, Mississippi was used in this research. Because the simulation includes both groundwater flow and contaminant transport, each calibration included both phases. The one-factor-at-a-time approach reduced the root-mean-squared (RMS) error criterion for the flow to 0.921225 feet in a total of 36 runs of Bioplume. The RSM approach reduced the error criterion to 0.918875 feet in a total of 47 runs. The one-factor-at-a-time approach was unable to reduce the RMS error criterion for the transport calibration below an initial value of 67.1831 parts per billion (ppb) benzene after 21 runs which spanned the feasible range of each of the parameters. The RSM approach was able to reduce the response to 67.0327 ppb after 47 runs of Bioplume. The RSM approach allows the modeler to identify parametric regions of improved response in a systematic way that would be extremely difficult to find using the one-factor-at-a-time approach. For this reason it may be very useful for calibration of Bioplume models to be used for research or long term monitoring of a contaminated site, where extra prediction accuracy may be needed. The major limitations of this work were the use of inefficient full factorial designs for the Response Surface Methodology approach and the limited improvement possible on the response surfaces possibly due to the assumption of homogeneous parameter values.

A COMPARISON OF RESPONSE SURFACE METHODOLOGY AND A ONE-FACTOR-AT-A-TIME APPROACH AS CALIBRATION TECHNIQUES FOR THE BIOPLUME-II SIMULATION MODEL OF CONTAMINANT BIODEGRADATION

I. Introduction

1.1 Motivation for Research

Groundwater simulation models are currently used to predict the effectiveness of various remediation schemes or the potential environmental and health threats posed by plumes of groundwater contamination. These models require parameter estimates and initial conditions in the form of field data before they can predict the future state vectors of groundwater hydrology and contaminant distribution. Groundwater models run with poor estimates of parameter values may result in inaccurate predictions of aquifer behavior, which may lead to counterproductive management decisions, wasted time and money, and even environmental and health consequences.

These problems might be avoided if the models used were better calibrated. Groundwater model calibration is a procedure for selecting parameter values which result in acceptable prediction accuracy. Professionals might be more willing to spend time on calibration if systematic and effective procedures were outlined for model calibration.

Response Surface Methodology (RSM) has been proposed as a calibration technique for groundwater contamination models (1) (19). RSM has not been compared to any other technique to determine whether it may represent a real improvement in terms of how many runs might be required for the method to converge or how closely it may calibrate a model.

1.2 Research Objectives

The goal of this research was to compare the Response Surface Methodology approach to the one-factor-at-a-time approach for calibrating the Bioplume II simulation model. This research was accomplished using the MADE-2 data from a natural gradient tracer experiment at Columbus Air Force Base, Mississippi (51). The measures used to compare the two calibration techniques were ease of use, number of runs required until improvement in response slowed significantly, and the best response found using each method.

II. Literature Review: The Inverse Problem

In general, simulation modeling involves the prediction of outcomes from a system. Many models may be formulated mathematically as:

$$\underline{X}_t = f(\underline{X}_0, \underline{\theta})$$

where \underline{X}_t is the future state vector of the system, \underline{X}_0 is a vector representing the current state of the system and $\underline{\theta}$ is a vector representing system parameters. How accurately the model predicts future states of the system is a function of the parameter set chosen to run the model. In groundwater modeling, as in many disciplines, direct measurement of parameter values may be difficult, expensive, or even impossible.

The problem of parameter estimation is the inverse problem of mathematics, where the parameter vector is solved for as the unknown. The inverse problem is often ill-posed in the sense that it does not lead to unique solutions and is unstable because small measurement errors result in large errors in parameter estimates (63:95). The nonuniqueness of the solution suggests that parameter sets that do not represent actual environmental parameter values may lead to successful calibration and even predict system response.

Anderson and Woessner (2:8) define calibration as the process of adjusting parameter values until model predictions match field data. This process involves minimizing the difference between the predicted final state of the system and the actual final state. This process requires the use of a historical data set, i.e. one which includes initial and final conditions for the site under consideration. Future states of the same system may be predicted after calibration has been completed. For example if data exists for years one and two, then the model may be calibrated using year one data as the initial condition and year two data as the final condition. Modeled values of year two data could then be compared to actual year two data and the difference between the two reduced via alteration of the input parameters.

Once this error has been minimized, the state of the system at year three may be predicted. In groundwater modeling, calibration is also called history matching.

A variety of solution techniques have been developed, including trial and error, direct methods, indirect methods, and the geostatistical approach.

2.1 Trial and Error

The trial and error approach is the most common technique in practice (16:199). This technique starts with an approximation of the parameter values as either fixed or spatially varying. The approximations may come from field measurements, literature values or experience. Bair and others (7:887-888) assumed literature values of effective porosity and then used trial and error adjustments for hydraulic conductivity. Rifai and others (47:1021-1023) performed calibration on the Bioplume II groundwater simulation model assuming constant hydraulic conductivity and recharge, obtaining aquifer thickness from well logs, and estimating the reaeration from the literature.

Trial and error is probably the dominant method due to its mathematical simplicity, but it may not be the best method overall. Keidser and Rosjberg (32:2219) note that the skill of the modeler plays a major role in efficiency and effectiveness of this method. Carrera and Neuman (16:199) note the method is time consuming and subjective.

2.2 Direct Methods

Yeh (63:96) defines the direct method (as classified by Neuman) or the equation error criterion (as classified by Chavent) to be the direct solution of flow and transport equations for parameters using measured and/or estimated data such as heads and concentrations. Willis and Yeh (57:352) state that this approach involves an explicit solution to an inverse boundary value problem where the parameter vector is treated as a dependent variable. Wise and Charbeneau (60:429) demonstrate the use of a direct semianalytical method to calculate parameter values based on field data. Butcher and Gauthier (14:73) applied a direct analytical solution to the inverse boundary value problem of determining the source geometry of a non-aqueous phase

layer. Statistical methods and iterative approaches may be coupled with direct methods, but in general the direct methods are characterized by their explicit solutions and lack of iterative technique. Their disadvantage is that the cumbersome mathematics behind the direct methods makes them awkward for solving complex problems.

2.3 *Indirect Methods*

Indirect methods, also called Output Error Criterion methods by Chavent refer to an iterative minimization of a norm of observed versus calculated data in order to approximate model parameters (63:96). Trial and error may be classified as an indirect method because it involves this successive approximation approach. Most indirect methods have an error criterion by which the goodness-of-fit of the parameter estimation is judged. Anderson and Woessner (2:238-241) describe three calibration criteria for matching simulated to observed groundwater head values: Mean Error (ME), Mean Absolute Error (MAE), and Root Mean Squared Error (RMS). The Mean Error is the average difference between simulated and observed values at data points (well nodes). Mean Absolute Error is average absolute value of the difference between simulated and observed values. Root Mean Squared Error is the square root of the average squared difference between simulated and observed values of head. The criteria are as shown in equations 1, 2, and 3 where n is the number of observation or well nodes, and the subscripts o and s represent observed and simulated values, respectively.

$$ME = \frac{1}{n} \sum_{i=1}^n (h_o - h_s)_i \quad (1)$$

$$MAE = \frac{1}{n} \sum_{i=1}^n |(h_o - h_s)_i| \quad (2)$$

$$RMS = \sqrt{\frac{1}{n} \sum_{i=1}^n (h_o - h_s)_i^2} \quad (3)$$

A response surface can be formed by the functional relationship between the parameter values and the error criterion selected. A relationship of the form $Y = f(\underline{\theta})$ would then be developed, where $\underline{\theta}$ is a vector of parameter values and Y is the response function.

Identification of an acceptable parameter vector is performed by moving along the response surface looking for an optimal response value.

A variety of methods have been developed to identify local minima. Devlin (25:327) demonstrated that Simplex optimization may be used to identify local minima of a response surface in order to estimate parameter values. Yeh and others (62:35) developed an iterative (indirect) parameter estimation routine involving two steps: (1) cokriging to estimate unknown parameter values and (2) steady-state simulation modeling with observed heads as constant, boundary values. Doughty and others (26:1741) developed an indirect technique to solve the inverse problem based on the use of fractals. Carrera and Neuman (17:218) describe a method to calculate optimal gradients to employ in the iterative method using a finite element approximation of the gradient of a least squares criterion including a head residual and a penalty function. Olsthoorn (42:44) proposed an indirect method to estimate parameter values by generating log parameter vectors, running the model, computing the error criterion, a jacobian matrix, and a gradient vector of the error criterion. The algorithm iteratively updates the parameter vector after each step. Freeze (27:751) noted that several statistical methods may be used to support indirect solutions to the inverse problem including weighted least squares estimation, bayesian estimation, and maximum likelihood estimation. Adams (1) and Cottman (19) demonstrated that Response Surface Methodology may be used to solve the inverse problem of flow model calibration by locating minima on a response surface using the sum of squared error criterion.

2.4 Geostatistical Approach

The geostatistical approach involves kriging and cokriging to estimate parameter values. Kriging is a statistical technique for optimal estimation of a spatially distributed parameter for which some values have been measured at a discrete points (observation wells). Cokriging is a related technique by which an unmeasured parameter's values are estimated from the values of a measured parameter which is correlated to the parameter to be estimated (24:323). Either of these techniques may be used to estimate parameter values from limited field data.

These techniques may also be used to fill data gaps where needed in connection with another calibration technique. Sun and others (52:90) used kriging to estimate parameters as continuously varying via measured point values and the use of a covariance matrix. Keidser and Rosjberg (32:2230-2231) compared four approaches to solving the inverse problem: kriging with prior data on response, kriging with zonation (establishing areas of constant parameter value), kriging alone, and zonation alone. They found that kriging with zonation resulted in the best model fit, except when data was scarce or there was large measurement error, in which case zonation alone was best. Freeze and others (27:751) explained that geostatistical approaches differ from other statistical methods to solve the inverse problem because they view parameters as spatially stochastic. Carrera and Glosorio (15:281) concluded that indirect statistical methods are superior to geostatistical methods.

2.5 Sensitivity Analysis

As stated earlier, the inverse problem is often unstable because small measurement errors generally result in large errors in parameter estimates (63:95). Errors in parameter estimates generally produce errors in predicted system response. Sensitivity analysis of parameter estimates is essential to determine the effect of parameter uncertainty on model prediction.

Sensitivity coefficients are the partial derivatives of response (head error or concentration error) with respect to each of the model parameters. Willis and Yeh (57:376) describe three methods of computing sensitivity coefficients: the influence coefficient method, the sensitivity equation method, and the variational method. The influence coefficient method was developed by Becker and Yeh (57:376) and involves altering parameter values and successively resolving the simulation model to observe the effect on model response. The sensitivity equation method involves taking the partial derivatives of the flow and/or transport equations with respect to each of the parameters and numerically solving for the sensitivity coefficients (57:377). The variational method, developed by Jacquard and Jain, Carter and others, and Sun and Yeh involves numerically estimating the coefficients using a triple integral over the subdomain of each node (57:378).

Other formal approaches have been developed to analyze sensitivity without the use of sensitivity coefficients. Keidser and Rosjberg (32:2219) suggest that if model parameters are random variables then statistical estimation and inference may be performed to assess reliability. Brooks and others (13:2996-2997) proposed a sensitivity analysis process for groundwater modeling based on using a simplex approach to identify extreme cases of model response based on variations in parameter values between feasible limits. Spear and others (49:3161) developed a method of parametric sensitivity analysis involving monte carlo simulation that allows variation of more than one parameter at a time. Yeh (63:103) cited Yeh and Yoon, and Shah and others who noted parameter uncertainty may be measured as the norm of the covariance matrix of estimated parameters.

2.6 *Parameterization*

Parameterization refers to the discretization of actual environmental variables into a given number of model parameters. The parallel concept of zonation is the assignment of zones of constant parameter value to model parameters. Carrera and Neuman (16:206) note that too many zones may increase error in parameter estimates. As parameterization increases system modeling error decreases, but parameter uncertainty increases (63:95). Sun and others (52:89) noted that because overparameterization may increase the variance of identified parameters, optimal parameterization is a balance between the error criterion (such as the residual of least squares error) and parameter uncertainty (measured for example by the covariance matrix of the estimated parameters).

Several approaches to parameterization have been developed. The simplest technique is to establish lumped parameter values which ignore spatial variations and assume the entire aquifer to be homogeneous (44:2). Yeh (63:98) explained that parameterization may be by zonation, where parameter values are constant over each zone, or by interpolation, where parameter values vary between nodes. In the finite element interpolation method (52:90) the parameter varies continuously via the basis functions which apply between sets of nodal values. In the stochastic inverse method (52:90) the parameter varies over a field via statistical

parameters and is estimated with the maximum likelihood approach combined with cokriging. Sun and others (52:101) propose parameterizing the model in connection with the geological characterization of the subsurface.

2.7 *Summary*

Extensive research has been completed on groundwater simulation model calibration. The problem is that many of these techniques have not been evaluated for efficiency. If a method is no more efficient than the trial and error approach, may not find support among modelers. Response Surface Methodology provides an example. This technique has been shown to work for calibration of groundwater simulation models (1) (19), but has not been demonstrated for contamination models or compared to other techniques. This thesis will evaluate the Response Surface Methodology to examine whether it may be more efficient or more effective than the baseline: one-factor-at-a-time or trial and error approach.

III. Background

3.1 Bioplume II

Bioplume II is a FORTRAN simulation model of the biodegradation of a contaminant in groundwater. It was written by Dr. Hanadi Rifai (46) (47) of Rice University as an alteration of the Method of Characteristics (MOC) finite difference model of fate and transport written by Konikow and Bredehoeft (34) at the USGS. The model simulates steady state or transient flow and both advective and dispersive transport, as well as both dissolved oxygen and hydrocarbon plumes. At the end of each time step, Bioplume II simulates the reaction between the two plumes using a mineralization ratio defined by the user. This approach differs from one where biodegradation is modeled using a simple decay term. The model is a standard in the field of environmental restoration and is commonly used to design remediation systems that utilize natural attenuation or injection of oxygenated water (48:55).

Bioplume II requires an input file which includes all the data that the model needs to simulate flow and transport. This input file contains values of constant and spatially varying parameters, such as porosity and hydraulic conductivity, as well as initial concentrations of oxygen and hydrocarbon contaminant. When Bioplume II is run, the system prints changing values of plume concentrations and other data related to the modeled groundwater system.

Bioplume II requires two layers of calibration because there are two layers of simulation. The hydraulic flow and the transport equations must both be considered. First a set of flow parameters are adjusted until the predicted hydraulic heads match the expected heads sufficiently. Second, a set of transport parameters are adjusted until the predicted concentrations are close to the expected final concentrations. After both steps are accomplished the calibration is complete.

3.2 Calibration Techniques

Two calibration techniques were compared in this thesis: a one-factor-at-a-time approach and the Response Surface Methodology (RSM) technique. The RSM technique in-

volves several procedures which can be used to locate the optimal response on an empirical response surface. RSM will be evaluated by comparing the number of runs required for calibration and the final degree of calibration via the Root mean Squared error criterion. The one-factor-at-a-time approach involves improving on the response, or fit, by iteratively changing one parameter at a time.

3.2.1 One Factor at a Time Calibration. The trial and error approach starts with an educated guess at each of the parameter values and then the modeler manually alters the parameters, one at a time, until an acceptable match, or fit, between the predicted and actual final conditions is achieved. In practice, trial and error is not any one standard approach, but the set of all manual iterative guessing calibration techniques. For the purposes of this work the trial and error technique means the one-factor-at-a-time approach.

To implement this approach, the parameters are listed in the order in which they are to be improved upon. Next the Bioplume II model is run at an initial parameter setting. The response for this parameter set is the error criterion for that point. The first parameter is then increased by a set amount, equal to the first significant digit (e.g. 32.7 would be increased to 42.7 or decreased to 22.7) and the model run again. If the initial parameter value is zero any reasonable step size may be chosen.

If the response does not improve, the parameter is decreased by the set amount to test in the other direction. If no improvement in response is found in either direction, then the parameter should be multiplied and then divided by increasing powers of ten until either a change in response is seen or the limit of a reasonable range for that parameter is reached. When the parameter improves, it is altered again in the direction of improving response.

This process is continued until response stops improving. The last three settings make two ranges which are then split in half. For example if the model was run for parameter x at $x = 1$, $x = 2$ and $x = 3$ and improved between one and two, but error increased for three, then the next step would be to split the two ranges and run the model at $x = 1.5$ and $x = 2.5$. The better of these two responses is chosen for further exploration with the ranges being split

in half at each step. Whenever two responses are equal, the choice of which one to further explore should be made randomly.

Once improvement in response ceases, the parameter is set at the last value for which improvement had continued and the procedure is repeated for the next parameter. This procedure is continued until the RMS response goes below some established cut off value. If all parameters are improved without meeting a termination criterion, the modeler goes through the list again beginning with the first parameter improved upon. If no improvement is seen after going through the whole list of parameters then the method may be seen as stalled.

3.2.2 Response Surface Methodology. Response Surface Methodology (RSM) is a technique for finding local optimal response values from an empirical model. The response in this case is a function of the difference between the predicted and actual final condition. The actual surface that RSM explores is the n -dimensional surface formed by assigning a response value to each coordinate point $(\theta_1, \theta_2, \dots, \theta_n)$, where θ_i is the value of the i th factor. Note that the value of this response surface could be determined at any point by running the model using the parameter values corresponding to the coordinate $(\theta_1, \theta_2, \dots, \theta_n)$ and calculating the error criterion for that run. This process allows the modeler to explore the surface at any point without knowledge of the nature of the response function $Y = f(\theta)$ itself. The RSM technique allows the modeler to examine a series of local approximations of the surface and move towards parameter regions of improved response. The method is based on the statistical fields of regression, analysis of variance, and experimental design. The actual process of RSM starts with a screening phase.

3.2.2.1 Screening Phase. The purpose of this phase is to determine which parameters significantly influence the response of the system. This process may be especially helpful when there are a large number of potential factors. Screening is generally accomplished by conducting experiments according to a Plackett-Burman or 2^{k-p}_{III} fractional factorial design, but may be performed less efficiently with a two-level full-factorial, or 2^k , design. A two-level full factorial design, for k factors contains every possible combination of the high and

low settings for the k factors $(\theta_1, \theta_2, \dots, \theta_k)$. For example if two parameters were under consideration, the model would be run at four different parameter combinations or coordinate pairs (θ_1, θ_2) because for $k = 2$, $2^k = 4$.

For convenience and ease of analysis the parameter values are linearly transformed into coded variables x_k :

$$x_k = \frac{\theta_k - \theta_{k0}}{S_k} \quad (4)$$

where θ_{k0} is the value of θ at the center of the design region and S_k is half the difference between the high and low levels of θ_k (the half-range of the region). The values of the coded variables are +1 for the high level and -1 for the low level.

The response values (error values from the experimental runs) are fit to a regression equation in the k -coded variables with or without interaction terms. For a three factor case the regression equation would be:

$$Y = \beta_0 + \beta_1 x_1 + \beta_2 x_2 + \beta_3 x_3 + \beta_{12} x_1 x_2 + \beta_{13} x_1 x_3 + \beta_{23} x_2 x_3 + \beta_{123} x_1 x_2 x_3 + e_i \quad (5)$$

Note that the error term in equation 5 is not random as is often the case with regression equations. In this work the error term is constant because the model is deterministic. If the same parameter set is used as input for Bioplume II in two different runs, the output will be the same. That is not to say there is no error: the response surface is an error surface, but the error is completely due to lack-of-fit. Therefore there is no pure error and the error surface is not stochastic.

The regression equation of the error surface indicates which factors have the most influence on the quality of the model calibration. Identification of these factors can be accomplished using a stepwise regression procedure or a normal probability plot. Since the deterministic nature of the data undermines the assumptions required by the standard t and F

test statistics, care must be taken when determining factor importance. Those factors accepted as influential are then considered in the first order design phase.

3.2.2.2 First-Order Design Phase. In the first order design phase, the response surface is assumed to be locally linear. RSM uses two level factorial designs to approximate the locally linear nature of the surface and a gradient search to locate a region of improved response. The process of generating an experimental design, fitting a first-order linear model, and conducting a gradient search continues until either the response is sufficiently low or significant improvement in response is not seen with further iterations.

If the first-order design does not converge on an acceptably low error value, then a second-order design may be needed. Refer to Box and Draper (12), for example, for more information on the second-order phase.

IV. Experimentation

4.1 Description

The evaluation of RSM as a calibration technique involved repeated calibration of the Bioplume II model using both RSM and the one-factor-at-a-time baseline approach. The calibration exercises involved:

1. Developing the Bioplume II input file from the data.
2. Developing Final Condition Grid from the data.
3. Performing a one-factor-at-a-time calibration on the simulation, documenting the number of runs required to complete the calibration, and recording the best response identified.
4. Performing an RSM calibration, documenting the number of runs, and recording the best response identified.
5. Comparing the one-factor-at-a-time approach to RSM.

Cottman (19) and Adams (1) used the RSM approach to calibrate a groundwater flow model. This work differs from that of Cottman and Adams in that the RSM calibration was conducted in two stages and compared to a baseline. The two stage calibration refers to the fact that two calibration surfaces exist: one for the flow calibration and the other for the transport calibration.

The initial parameter values chosen for each phase of the calibration (i.e. flow or transport) were selected from the feasible range of each of the parameters under consideration. The parameters under consideration for the flow calibration were the hydraulic conductivity, the porosity, and the diffuse recharge rate. The parameters adjusted for transport calibration were longitudinal dispersivity, ratio of longitudinal to transverse dispersivity, stoichiometric ratio (for biotic reaction between oxygen and benzene), retardation factor and reaeration coefficient.

The actual calibration using either technique required the use of an error criterion. In this work, the root mean square (RMS) criterion was selected because it was hoped that it would yield a more linear response surface than that posed by the SSE criterion used by Cottman (19).

4.1.1 Mathematical Setting of the Problem. The mathematical problem solved in this research is the inverse problem of mathematics, discussed in chapter 2. Specifically, the parameters for the Bioplume-II model are estimated using an empirical response function. The error generated by estimating model parameters was minimized using both the one-factor-at-a-time and RSM approaches.

The Root Mean Squared Error is a function of the difference between the simulated final condition and the actual final condition (kriged from real data in this case). The simulated final condition may be found for any combination of parameter values, θ by running the simulation model, Bioplume-II. The domain of the problem is the $n + 1$ dimensional space formed by the n factors being calibrated and the error response. The boundaries of the domain are the range of feasible values of each parameter found in the literature. The initial condition is provided by field data from the MADE-2 site. The boundary conditions of the simulation model are constant hydraulic heads based on field data: a first-order boundary condition.

To simplify the solution homogeneity was assumed for all factors that were calibrated. Isotropy was assumed for all factors except dispersivity, which was dealt with in the calibration. To the degree that these were poor assumptions, additional error was introduced.

4.2 Conduct

The experiment required construction of an input file, determination of a final condition and both flow and transport calibration using the one-factor-at-a-time approach and the RSM approach.

4.2.1 Input File Preparation. The preparation of the input file involved obtaining the MADE-2 data set, developing the finite difference grid, determining an acceptable time step, and constructing the input file.

4.2.1.1 Data. The first step was to develop a Bioplume II input file from the data provided by Dr. Stauffer on the MADE-2 site (51) (50). The data from the site was measured in three dimensions. Bioplume-II simulates only two dimensions, however, so some data had to be transformed via vertical averaging. The data set included hydraulic conductivity, dissolved oxygen, contaminant concentrations, and water surface elevations. Readings were available from June 1990 through September 1991. The input file represents the condition at the site in June 1990. Bioplume was used to "predict" conditions in September 1991. These predicted values were then compared to the measured data from September 1991. The precision of the measurements and the uncertainty in the data from the MADE-2 site are not important in this research because the goal is to compare the two methods of calibrating the model. If any conclusions were to be drawn from the field data itself, then the quality of the data would be more important.

Only parts of the data were needed. The hydraulic conductivity was altered as one of the calibration parameters, and was represented as a single homogeneous value. Because of this simplification, a rough average value was all that was needed to represent that parameter. This simplification would also lead to an increase in the minimum value of the error response. This had profound implications for the comparison between the two methods because the techniques were limited in how well they could calibrate the model. Because Bioplume II has the capability to model injection of contaminants, initial plume data was not needed. The initial water surface profile and dissolved oxygen values (50:89-96) were important, but before they could be added to the input file, a finite difference grid had to be developed onto which values could be placed.

4.2.1.2 Grid Design. The maximum grid size that Bioplume-II allows is 20 x 30 nodes. This size was chosen to increase the accuracy of the modeling; in general denser

grids exhibit reduced error. Due to the size of the site, a 10 x 10 meter cell seemed appropriate, but two factors complicated the grid spacing.

First, the extent of plume spreading was not as large as the site. After benzene was selected as the contaminant to be modeled, the grid size was reduced in order to minimize the size of the modeled region, while still capturing the entire benzene plume. Those water table and dissolved oxygen data points outside the region of the benzene plume's maximum extent were deleted and the remaining points were used to construct the data set with the Surfer (31) software package.

The second factor was that the Surfer software used to approximate the values of spatially varying groundwater variables (31) can only view the nodes as intersections on a grid, not as cells of the type used by a finite difference model. To use Surfer the intersections must be viewed as the centers of the finite difference nodes. Surfer then calculates the length and width of the cells by dividing the total dimension by the number of internodal spaces. For twenty nodes, Surfer uses twenty grid intersections and has nineteen internodal spaces. For thirty nodes Surfer has twenty-nine internodal spaces.

The final length and width of the modeled region was set automatically by Surfer to the range of well coordinates that were included after the data point reduction described above. The total length was 391.1724 feet and the total width was 367.357 feet, with the injection well at 196.144 feet by 81.1144 feet from the corner of the modeled region. The placement of the well was based on the actual location of injection wells at the MADE-2 site (50). Therefore, as shown below, the longitudinal length of the nodes was set to 13.49 feet and the transverse dimension of the cells to 19.33 feet.

$$\frac{(367.357 \text{ meters})(3.28 \text{ ft/m})}{19 \text{ spaces}} = 13.49 \text{ feet}$$

$$\frac{(391.1724 \text{ meters})(3.28 \text{ ft/m})}{29 \text{ spaces}} = 19.33 \text{ feet}$$

The injection well was then placed at 11 nodes in the x-direction ($\frac{196.144}{19.33} \approx 11$) and 23 nodes in the y-direction ($\frac{81.1144}{13.49} \approx 7$) from the corner of the modeled region.

In order to ensure stability, the nodal discretization needed to be acceptably fine. A maximum nodal length in the flow direction could be calculated via the cell Peclet Number (Pe_c) as:

$$Pe_c = \frac{\text{advection}}{\text{dispersion}} = \frac{\nu \Delta y}{D_L} = \frac{\nu \Delta y}{\alpha_L \nu} = \frac{\Delta y}{\alpha_L}$$

where

Pe_c = Cell Peclet Number

ν = Groundwater Velocity

Δy = Longitudinal Length of Cell

α_L = Longitudinal Dispersivity

D_L = Longitudinal Dispersion Coefficient

The cell Peclet number should be no more than two to ensure numerical stability (61:65). As seen in equation 8 the node length in the direction of flow should be no more than twice the longitudinal dispersivity.

$$Pe_c \leq 2 \quad (6)$$

$$\frac{\Delta y}{\alpha_L} \leq 2 \quad (7)$$

$$\Delta y \leq 2\alpha_L \quad (8)$$

Young and Boggs (64:11-15) estimated longitudinal dispersivity at the site to be between 10 and 42 meters. Mercado (39) suggested estimating longitudinal dispersivity, α_L , as:

$$\alpha_L = \frac{1}{2} \left(\frac{d_d}{P_{avg}} \right)^2 L_d \quad (9)$$

where

P_{avg} = Average Value of Permeability

d_d = Standard Deviation of Permeability

L_d = Mean travel Distance

Boggs and others (10:3282) present permeability distributions for four core samples from the MADE-2 site. They also note the tracer plume traveled about 280 meters in 594 days (10:3288). A value of 36.3 feet, calculated via equation 9, is within the range prescribed by Young and Boggs (64:11-15) though at the low end of that range (10 meters = 32.8 feet). That value is acceptable however because a smaller value of α_L is more conservative in terms of nodal discretization because it should lead to a finer grid. Keeping Δy below twice the longitudinal dispersivity, the maximum longitudinal length of a node is 72.6 feet. This value is safely above the value of 13.49 to be used in this work.

4.2.1.3 Time Step. The length of the time step also impacts numerical stability. A shorter time step increases accuracy, but can increase computer time. A simple equation can be used to calculate a maximum time step. For stability of the algorithm the value of ν , the Courant number, defined by $\nu = \frac{v\Delta t}{\Delta y}$, where v equals the velocity of groundwater, should be no more than one (61:65). Solving for Δt in this equation yields:

$$\Delta t = \frac{\nu \Delta y}{v}$$

Given that $\nu \leq 1$:

$$\Delta t \leq \frac{\Delta y}{v}$$

when $\Delta y = 10$ meters:

$$\Delta t \leq \frac{10 \text{ meters}}{v}$$

Velocity can be estimated from measured tracer plume movements of approximately 160 meters in 503 days and 280 meters in 594 days for rates of 0.318 and 0.471 meters per day (10:3287-3288).

Therefore:

$$\Delta t \leq \frac{10 \text{ meters}}{0.471 \text{ meters/day}} \quad (10)$$

$$\Delta t \leq 21.2 \text{ days} \quad (11)$$

The maximum time step should therefore be 21.2 days in order to maintain numerical stability. Bioplume allows the modeler to set up multiple pumping periods which can each have different length time steps. In order to model the injection, an initial pumping period was needed which coincided with the injection time. Once the injection time was over, the remaining time could be divided evenly into any convenient units. Since the injection took two days, two one-day time steps were included in the first pumping period. The remaining time was divided into five pumping periods of 92 one-day time steps each. These time steps directed the computer to model the fifteen month period with time steps much smaller than the 21.2 day maximum required for numerical stability.

4.2.1.4 File Assembly. Surfer was used to set up the Bioplume-II input file by estimating initial values of dissolved oxygen and water table elevation for each finite difference node. Other characteristics of the initial site condition were set to specific values. The transmissivity was set to 0.00226042 square feet per second based on an approximation of the hydraulic conductivity from the data divided by 1.96 feet of depth. The 1.96 feet was both the aquifer screening length and the modeled depth of the aquifer. Injection wells were set to values given in Boggs (9:2-1). In most cases, the value for leakance, recharge of water to the aquifer, was set to zero. At the upstream and downstream ends, however, the leakance parameter was set to keep the heads constant for a first order boundary condition.

The hydraulic flow modeling was assumed to be steady state. To test this assumption, Surfer was used to draw contour maps of the water table surface over the time period to be modeled. The contour maps confirmed the acceptability of the steady state assumption. They indicated that for the time period under consideration at the site, the hydraulic gradients did not change significantly. For more information on the structure of the input file, refer to Rifai (46). The initial input file is included as Appendix B.

4.2.2 Final Condition. To determine if the model was calibrated after a given run, the output from that run was compared to the final condition given in the original data. To facilitate this comparison, the Surfer software was used to estimate both the initial and final water table elevation and contaminant concentration for each finite difference node. The RMS error of the differences between the heads or concentrations over the entire finite difference grid was calculated for a given run of Bioplume-II using the FORTRAN program listed in Appendix D.

4.2.3 One-Factor-at-a-Time Approach. The one-factor-at-a-time calibration consisted of two phases: the flow calibration and the transport calibration.

4.2.3.1 One-Factor-at-a-Time Flow Calibration. The first parameter varied, chosen arbitrarily, was the transmissivity. Starting with the nominal value of 0.00226042

mentioned in paragraph 4.2.1.4, the transmissivity was incrementally varied. The goal was to minimize the error criterion by varying the value, within a reasonable range.

Table 1 shows the values used and the resulting error values. The range of transmissivities considered was based on the feasible range of hydraulic conductivities in the United States (56:8). Walton lists 0.001 ft per day through 10,000 ft per day as the range for hydraulic conductivity in the United States. The range for the transmissivity values was based on the fact that transmissivity can be expressed as the product of aquifer depth and hydraulic conductivity, as depicted in equation 14. The aquifer was modeled as 1.97 feet deep, which was the depth of the screened portion of the injection well. Therefore the transmissivity was 1.97 times the hydraulic conductivity. Transmissivity variation was bounded between 2E-8 and 0.228 ft²/sec, as depicted in equations 14 and 15.

<i>Run No.</i>	<i>Transmissivity (ft/sec)</i>	<i>RMS flow</i>
1	2.26042E-3	2.23746
2	3.26042E-3	2.23746
3	1.26042E-3	2.23746
4	2.26042E-2	2.23746
5	2.26042E-4	2.23746
6	2.26042E-1	2.23746
7	2.26042E-5	2.23746
8	2.26042E-6	2.23746
9	2.26042E-7	2.23746
10	2.26042E-8	2.23746

Table 1. Values of Transmissivity and RMS Error

$$T = Kb \quad (12)$$

$$\left(\frac{0.001 \text{ft}}{\text{day}} \right) \left(\frac{1 \text{day}}{86400 \text{sec}} \right) (1.97 \text{ft}) = 2 * 10^{-8} \text{ft}^2/\text{sec} \quad (13)$$

$$\left(\frac{10000\text{ft}}{\text{day}}\right) \left(\frac{1\text{day}}{86400\text{sec}}\right) (1.97\text{ft}) = 0.228\text{ft}^2/\text{sec} \quad (14)$$

Table 1 shows that increasing and decreasing the transmissivity by 1.0E-3 from its initial value of 2.26042E-3 did not alter the error criterion for the flow calibration. The value remained at 2.23746 feet, regardless of the value of the transmissivity parameter. Scaling the transmissivity up and down by powers of ten also did not change the value of the error criterion for the flow calibration.

The second parameter varied was porosity. Boggs and others describe the aquifer as "sandy gravel and gravelly sand" (10:3282). Walton lists a range of reasonable permeabilities for a sand and gravel aquifer as 0.20 through 0.35 (56:413). Boggs and others (10:3282) took samples at the site and determined that the porosities at the site had either a mean of 0.30 with a standard deviation of 0.07 or a mean of 0.32 with a standard deviation of 0.09. To include a wide range of reasonable values the porosity calibration was bounded between 0.20 and 0.41. The results of the porosity calibration are shown in Table 2. These results show that the variation of porosity within a reasonable range did not reduce the error criterion.

<i>Run No.</i>	<i>Porosity</i>	<i>RMS flow</i>
11	0.215	2.23746
12	0.410	2.23746

Table 2. Values of Porosity and RMS Error Criteria

The third parameter varied was the recharge rate. There was no data available on a reasonable range for the recharge rate, so the model was started with a few values to determine which might yield a good initial value. Simulation time was used to determine a feasible starting value for this parameter. To predict how much CPU time the simulation would require for a given run, the number of particle moves required per time-step was recorded for several runs. Any value more than approximately 50 moves was prohibitive in terms of time to run and memory requirements. Therefore the recharge rate was changed from zero to 5E-7 feet per second. Refer to the Bioplume II manual for more information on particles in Bioplume

II (46:7-6). Table 3 shows the number of particle moves per time step required by Bioplume II for several diffuse recharge rates as displayed by Bioplume II.

<i>Diffuse Recharge in feet per second</i>	<i>Required Particle Moves Per Time Step</i>	<i>Estimated Run Time</i>
5E-3	58086	300 days
5E-4	5809	30 days
5E-5	581	3 days
5E-7	7	1 hour

Table 3. Diffuse Recharge and Required Particle Moves

A somewhat arbitrary range of -1E-6 through 5E-6 was established, based on computer limitations described above. Results of the calibration using diffuse recharge are shown in Table 4. Note that recharge is negative discharge. The results are also displayed in graphical form in Figure 1.

<i>Run No.</i>	<i>Diffuse Discharge in feet per second</i>	<i>RMS flow</i>
13	-5E-7	4.54487
14	5E-7	0.990886
15	1E-6	2.92961
16	7.5E-7	1.82458
17	2.5E-7	120544

Table 4. Diffuse Discharge and RMS Error Criteria

Clearly, the hydraulic heads are most sensitive to the recharge/discharge parameter when compared to the other parameters studied. The discharge was set to 5E-7 feet per second, and since all three flow parameters had already been tried, transmissivity was randomly selected to be recalibrated. During the recalibration of transmissivity, its variation affected response. These results are shown on Table 5 and displayed graphically in Figure 2. The best transmissivity parameter value selected was 2.76042E-3 feet/second with an RMS value of 0.921225 feet.

Because the transmissivity recalibration did not bring the error criterion below a desired cutoff value of 0.5 feet the calibration was continued. Porosity was randomly selected for

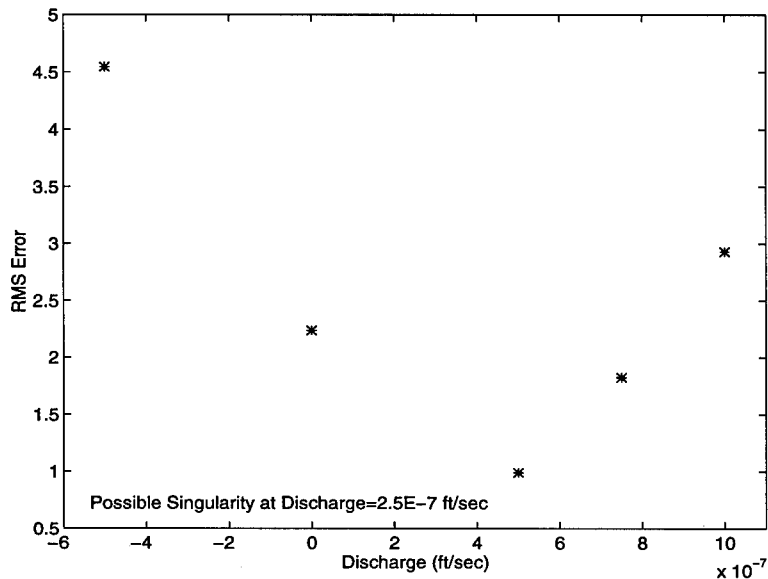


Figure 1. RMS Error vs. Diffuse Discharge Rate

recalibration. The results of the porosity recalibration are shown in Table 6. Variation of porosity once again did not affect the error criteria.

Because the range of reasonable porosity values does not permit expansion by a factor of ten in either direction, recalibration on porosity was complete. Discharge was randomly selected for recalibration by assigning ranges to each factor and using a random number generator.

Run No.	Transmissivity (ft/sec)	RMS flow
18	3.26042E-3	0.990044
19	4.26042E-3	1.19303
20	3.76042E-3	1.09244
21	2.76042E-3	0.921225
22	2.51042E-3	0.928127
23	3.01042E-3	0.947168

Table 5. Recalibration on Transmissivity

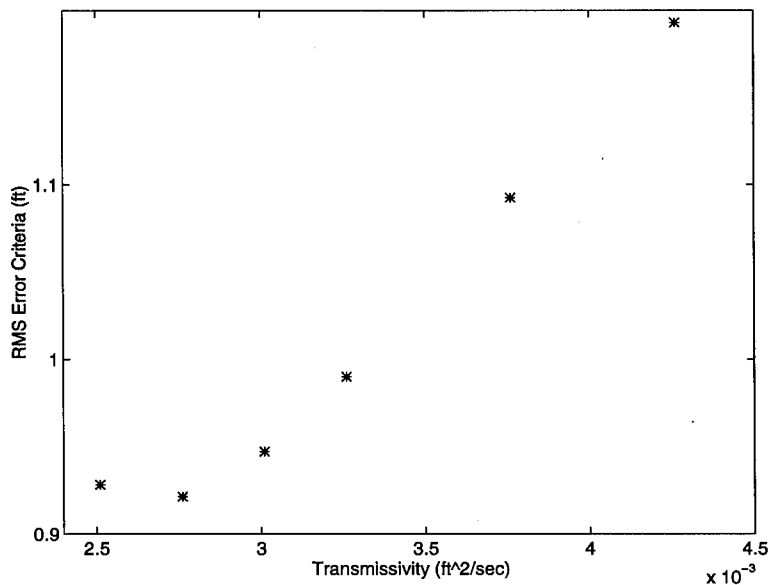


Figure 2. RMS Error vs. Transmissivity

Run No.	Porosity	RMS flow
24	0.215	0.921225
25	0.410	0.921225

Table 6. Recalibration on Porosity

The discharge recalibration began with the current 5E-7 feet per second and moved a step in both directions. Because no improvement was identified in the response an order of magnitude jump would have been taken in both directions. Due to CPU time and memory restrictions the jump could only be taken in the direction of smaller values. The largest value used was 1E-6 feet per second.

The results of the discharge recalibration are shown in Table 7 and displayed graphically in Figure 3. Even with this jump no improvement was found. Due to lack of progress the one-factor-at-a-time flow calibration was determined to be completed at this point and the transport calibration begun.

Run No.	Diffuse Discharge (ft/sec)	RMS flow
25	5E-7	0.921225
26	1E-6	2.11809
27	0.0	2.23746
28	5E-8	2.05905

Table 7. Recalibration on Discharge

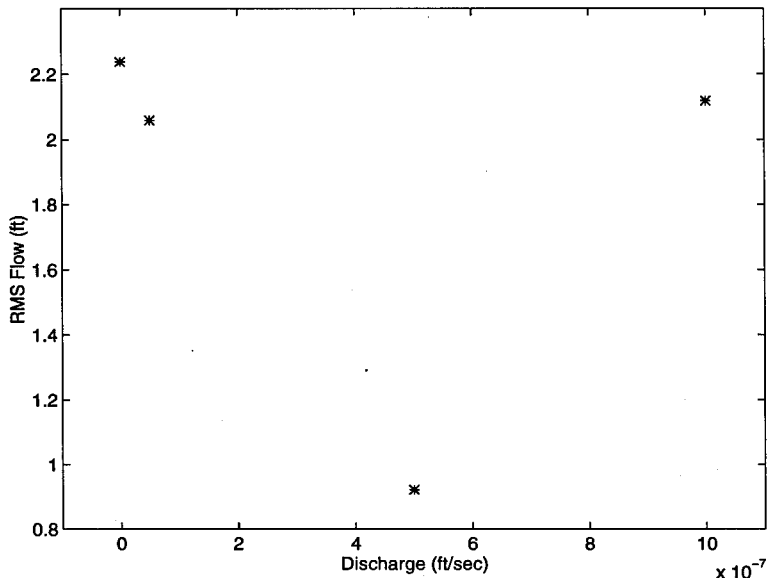


Figure 3. RMS Error vs. Discharge

With the completion of calibration by transmissivity, porosity and diffuse recharge, the flow calibration was completed. In a total of 28 runs the RMS flow criteria was reduced to 0.921225 feet.

4.2.3.2 One-Factor-at-a-Time Transport Calibration. After the flow calibration was completed, the transport calibration was begun. The first parameter varied was the longitudinal dispersivity. Hess cites Young and Boggs (64:2012) who performed field experiments on the MADE-2 site to approximate the longitudinal dispersivity to be between 10 and 42 meters (32.8 and 137.76 feet). Using these values as the reasonable range, the

calibration was continued. Table 8 presents the results, which show that the variation of longitudinal dispersivity did not change the error criteria.

<i>Run No.</i>	<i>Longitudinal Dispersivity</i>	<i>RMS transport</i>
1	46.3	67.1831
2	32.8	67.1831
3	56.3	67.1831
4	137.76	67.1831

Table 8. Values of Longitudinal Dispersivity and RMS Error

The second parameter varied was the ratio of longitudinal to transverse dispersivity. This value had been held at 0.4, but was then varied between the limits suggested in the Bioplume manual (46:7-15) of 0.001 through 1.0. The results of calibration on this ratio are shown in Table 9 and demonstrate that varying the value of transverse dispersivity did not change the response of the model.

<i>Run No.</i>	<i>Ratio of Longitudinal to Transverse Dispersivity</i>	<i>RMS transport</i>
5	0.5	67.1831
6	0.3	67.1831
7	1.0	67.1831
8	0.04	67.1831
9	0.004	67.1831

Table 9. Ratio of Longitudinal to Transverse Dispersivity and RMS Error

The third parameter varied was the stoichiometric ratio for reaction between oxygen and hydrocarbon under aerobic biodegradation. This value is the ratio of oxygen to carbon atoms required for biodegradation of benzene. In the case of complete mineralization of benzene to carbon dioxide and water, the ratio may be calculated exactly from the stoichiometric equation for aerobic mineralization of benzene shown below (48:56). Note that fifteen oxygen atoms are needed for every six carbon atoms. The stoichiometric ratio is therefore 15/6 or 2.5. The value must be calibrated because full mineralization of the benzene may not occur over the modeled time period. This value was varied between 2 and 4 based on the recommendation of Dr. Rifai (45). The results of calibration on the stoichiometric ratio are shown in Table 10.

Run No.	Stoichiometric Ratio	RMS transport
10	4.0	67.1831
11	2.0	67.1831

Table 10. Stoichiometric Ratio and RMS Error

The fourth parameter to be varied was the Retardation Factor. This factor represents the delay in spreading of the contaminant plume caused by adhesion to the soil matrix and is defined as shown in equation 17. The value of θ_W , percent saturation, is unity in this case because the simulation models the saturated zone. Simplification results in equation 19. Before this point, the Retardation Factor was given a value of one. This assumption, in effect, stated that K_D , the distribution coefficient of the aquifer or ρ_B , the bulk density of the solid matrix, was zero.

$$R_f = 1 + \frac{\rho_B K_D}{\theta_W} \quad (15)$$

$$R_f = 1 + \rho_B K_D \quad (16)$$

$$K_D = \frac{R_f - 1}{\rho_B} \quad (17)$$

Stauffer and others (50:75) list a mean value of retardation of 1.20 for the site with a standard deviation of 0.20. Arbitrarily taking plus or minus one standard deviation as a reasonable range for the factor, retardation was allowed to vary between 1.00 and 1.40. Because Bioplume treats retardation as a function of ρ_B and K_D this range had to be reflected in their values. Bulk density was set to 1.77 grams per cubic centimeter, a mean value from field data (50:5). Equation 19 was then solved for K_D as shown in equation 20. This equation was then used to find a range for the Distribution Coefficient given the range for the Retardation Factor. The range selected for the Distribution Coefficient was [0.00, 0.22599]

with units of cubic centimeters per gram. The results of the variation of retardation factor were uninteresting. Five values of K_D were tried with the same result for each run as shown in Table 11.

<i>Run No.</i>	<i>Distribution Coefficient</i>	<i>RMS transport</i>
12	0.11299	67.1831
13	0.21299	67.1831
14	0.01299	67.1831
15	0.22599	67.1831
16	0.01299	67.1831

Table 11. Distribution Coefficient and RMS Error

The last transport calibration factor to be tried was the reaeration coefficient. Five values of this factor were used as shown in Table 12.

<i>Run No.</i>	<i>Reaeration Coefficient</i>	<i>RMS transport</i>
17	1.184E-3	67.1831
18	2.184E-3	67.1831
19	0.184E-3	67.1831
20	5E-3	67.1831
21	1.184E-4	67.1831

Table 12. Reaeration coefficient and RMS Error

Once again, variation of this factor did not lead to variation in the response. Each time the model was run, the results were the same: RMS transport was 67.1831. Due to lack of progress the one-factor-at-a-time flow calibration was determined completed, having made no progress after 21 runs of the model.

4.2.4 RSM Approach. The second calibration procedure used was the Response Surface Methodology technique. This procedure involved three distinct phases. The screening phase is designed to determine if any factors are insignificant and may be eliminated from further consideration. The first-order phase uses an empirical first-order regression model to approximate the true response surface and find parameter combinations that lead to optimal

response values. The final phase is the second-order phase in which second-order regression models are used to improve the empirical model and find optimal parameter combinations.

4.2.4.1 RSM Flow Calibration. The RSM flow calibration consisted of the three phases described above.

Screening Phase of RSM Flow Calibration. The screening design included three factors: the transmissivity, porosity and diffuse discharge. A full factorial design was used because of its simplicity. Eight runs (2^3) runs of Bioplume were used to determine which factors, if any, could be excluded from the analysis.

These runs were performed at all possible combinations of high and low levels of the range of each parameter. The levels are shown in Table 13. Due to the cost in terms of CPU time and memory, the discharge could not be set with an absolute value higher than 1E-6. Transmissivity settings above 0.0228 also caused problems with CPU time and memory. These values were high enough, however, to provide a sufficient range for the screening design. The results of the eight runs are shown in Table 14.

Factor	Low-Level	High-Level
Transmissivity	2E-8	0.0228
Porosity	0.20	0.41
Discharge	-1E-6	1E-6

Table 13. Levels of Flow Parameters

Once the runs were completed they were evaluated using regression. A stepwise procedure adds and deletes one factor or interaction term at a time in the regression equation to determine whether the term improves the fit of the regression. Only those terms significantly improving the fit are included at each step. This procedure was used to determine which factors, including interactions, were worth keeping in the analysis. Since the Bioplume-II model produces deterministic output, the statistical significance of the regression model or of any individual factors was not meaningful. SAS was, however, still able to provide a least squares model of the error response. The stepwise procedure approximated a parsimonious

Run No.	Transmissivity	Porosity	Discharge	RMS flow
1	2E-8	0.20	-1E-6	27246.5
2	2E-8	0.20	1E-6	544968
3	2E-8	0.41	-1E-6	27246.5
4	2E-8	0.41	1E-6	544968
5	0.0228	0.20	-1E-6	2.22
6	0.0228	0.20	1E-6	1.81
7	0.0228	0.41	-1E-6	2.22
8	0.0228	0.41	1E-6	1.81

Table 14. Screening Design and RMS Error

model, using the coded, i.e. transformed, data rather than the actual parameter values. The resulting regression model revealed that neither porosity nor any of the interaction terms that included porosity were worth including in the calibration. The stepwise procedure from SAS is shown in Appendix C-1.

First-Order Design Phase of RSM Flow Calibration. The First-Order design phase of RSM was used with only the two significant factors from the screening design: transmissivity and discharge. Given that a full factorial, 2^k design was used for these two factors, four runs of Bioplume were needed for each design used. The high and low settings for the first-order design phase differed from those of the screening phase. In the screening phase, the settings spanned the range of reasonable values for the variable. In the first-order design phase, they represented a range around the current setting. A range of $\pm 80\%$ of the initial value was used (19:4-13). The results of the first run of the first-order design phase are shown in Table 15.

Run No.	Transmissivity	Discharge	RMS flow
9	4.068756E-3	5E-8	2.11605
10	4.068756E-3	-5E-8	2.36023
11	4.52084E-4	5E-8	1.24133
12	4.52084E-4	-5E-8	3.37311

Table 15. First Run of the First-Order Design Phase and RMS Error

These results were modeled in a first-order linear regression equation using SAS. The regression output from SAS is shown in Appendix C-2. The SAS output shows that the fit was poor, with an R^2 value of 0.6139. In order to develop a more reliable model (that could be trusted) the design size was reduced to $\pm 40\%$ of the factor's value. A centerpoint value of 8.401E-7 was randomly selected for discharge because a range around a value of zero could not be based on a percentage. The results of runs from this design are shown in Table 16.

<i>Run No.</i>	<i>Transmissivity</i>	<i>Discharge</i>	<i>RMS flow</i>
13	1.356252E-3	5.0406E-7	2.21077
14	1.356252E-3	1.176E-6	7.46751
15	3.164588E-3	5.0406E-7	0.967852
16	3.164588E-3	1.176E-6	2.21034

Table 16. Second Run of the First-Order Design Phase and RMS Error

These results were also fit to a first-order regression equation using SAS. The R^2 value was an improved 0.8398, but the F-ratio was 2.622. The F-test has no meaning here because it is based on an assumed normal error distribution around each response value. Although the response surface is an error surface, the error is deterministic and so the normal assumption can not hold. The F-ratio is the amount of the total sum of squared response which is explained by the model divided by that attributed to lack of fit. Therefore any value over 1.0 means more of the sum of squares is explained by the model than is attributed to lack of fit. The higher the F-ratio, the better the fit. The regression output is shown in Appendix C-3.

The second attempt to develop a significant model was the addition of a center point to the 2^k design. This made for a total of five data points. The fifth data point is shown in Table 17.

<i>Run No.</i>	<i>Transmissivity</i>	<i>Discharge</i>	<i>RMS flow</i>
17	2.26042E-3	8.401E-7	2.21077

Table 17. Centerpoint of Previous Design and RMS Error

The fifth data point did not improve the R^2 value, but it did increase the F-ratio to 4.370. This was thought to be acceptable for developing a gradient vector. The regression output is shown in Appendix C-4. The coefficients of the regression equation were used to calculate the elements of the gradient vector. The vector desired was the vector of steepest descent, which is based on the additive inverses of each element. The elements had to first be normalized to establish the unit gradient vector. Then the values were decoded because they were based on the transformed coordinate system, where the center of the current design had coordinates of $(0, 0)$.

The transformation followed equation 4, which was solved for θ_k , as shown in equation 20. Note that x_k is the coefficient value, in coded units, from the regression equation. S_k is the half range of the region in standard units and θ_{k0} is the value of the parameter, in standard units, at the center of the design region. The results are shown in Table 18.

$$\theta_k = x_k S_k + \theta_{k0} \quad (18)$$

Factor	Regression Coefficient	Normalized Coefficient	Uncoded Value
Transmissivity	-1.625022	-0.707154	1.6210E-3
Discharge	1.624807	0.707060	1.0777E-6

Table 18. Table of Calculations for Steepest Descent Gradient

The uncoded values, which were the elements of the uncoded steepest ascent gradient vector, were then subtracted from the parameter values at the center of the design region. The new coordinate represented a single step along the gradient vector. A new test at this point revealed that the design region had been too large. The response at the unit step was worse than before, when it was expected to have generated an improved response. The new response is shown in Table 19 as run number 18.

Using the same design, the step size was decreased in the direction of the gradient vector. Instead of moving one unit vector in the gradient direction, a new test point was established at 50% of the steepest descent gradient vector. This test point revealed a response

of 0.941898 for flow calibration. This value was an improvement over the response at the center of the first design, 2.21077 feet. Values at 40 and 60% of the unit step were taken to determine whether the 50% step led to the best response along the gradient vector.

Run No.	Step Number	RMS Flow
17	Center of First Design	2.21077
19	4/10	1.16225
20	5/10	0.941898
21	6/10	1.01111
18	Unit Step	6.15908

Table 19. Table of RMS Flow Values along First Gradient Vector

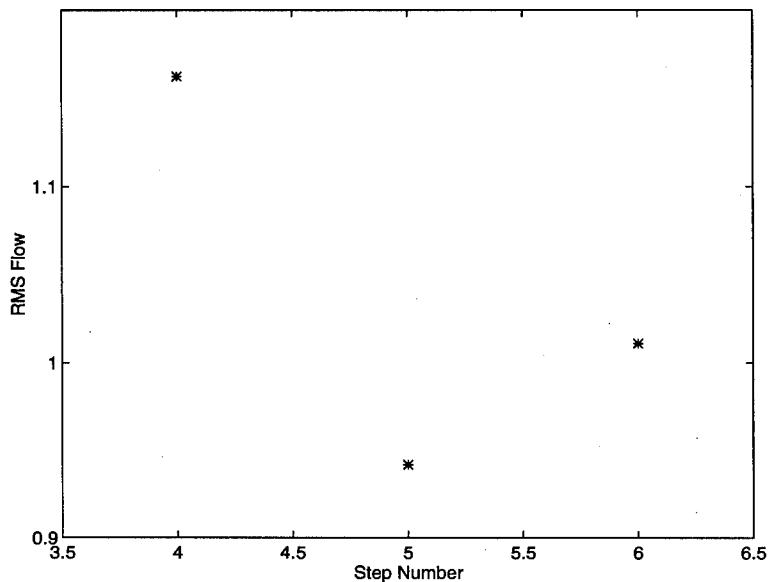


Figure 4. Graph of RMS Flow Along Gradient Vector

Once the 50% step was chosen as the low point along the descent path a new design was established. The first design, centered on the 50% step, that led to an F-ratio over two was at $\pm 5\%$ of the parameter values. These results are shown in Table 20. It had an F-ratio of 5.821 and an R^2 value of 85.34%, see Appendix C-5 for the SAS output from this design.

<i>Run No.</i>	<i>Transmissivity</i>	<i>Discharge</i>	<i>RMS flow</i>
22	1.39E-3	2.86E-7	0.940928
23	1.39E-3	3.16E-7	1.01783
24	1.53E-3	2.86E-7	0.918875
25	1.53E-3	3.16E-7	0.942795

Table 20. Run of a 5% Design Centered on 5th Step

The next step was to calculate the steepest descent gradient from this point. Using equation 20, the steepest descent gradient was calculated from the coefficients of the regression equation. The results of these calculations are shown in Table 21.

The unit gradient step was not the first step used for the gradient search here because the unit gradient step would have been beyond the feasible region for transmissivity. Instead, in an attempt to explore the first-order design further, 10% steps were taken. Then step ten was taken in the direction of the discharge component of the steepest descent gradient vector. This tenth step is the gradient search subject to a constraint as outlined in Box and Draper (12). The results of the Bioplume II runs are shown in Table 22. Note that the unit gradient step was taken at step nine was the last step that could fit within the range of acceptable values for transmissivity. See Figure 5 for a graph of the progress made along the gradient vector.

<i>Factor</i>	<i>Regression Coefficient</i>	<i>Normalized Coefficient</i>	<i>Uncoded Value</i>
Transmissivity	-0.024272	0.6936	1.511E-3
Discharge	0.025206	0.7203	3.118E-7

Table 21. Table of Calculations for Second Steepest Descent Gradient

Finally a 5% design around the ninth step along the last gradient vector was tried. This design had results shown in Table 23. The SAS analysis of this first-order design showed an F-ratio of 1.840 and the R^2 value was only 0.6479. See Appendix C-6 for these results.

Second-Order Design Phase of RSM Flow Calibration. Because this design was already so small, a second-order design was appropriate at this stage. Again the reader should consult Box and Draper (12) for more information on second-order strategies.

<i>Run No.</i>	<i>Step Number</i>	<i>RMS Flow</i>
20	Center of Second Design	0.941898
26	1	0.941433
27	2	0.940855
28	3	0.940116
29	4	0.939734
30	5	0.939193
31	6	0.938374
32	7	0.936984
33	8	0.934117
34	9	0.925218
35	10	3.30866

Table 22. Table of RMS Flow Values along Second Gradient Vector

<i>Run No.</i>	<i>Transmissivity</i>	<i>Discharge</i>	<i>RMS flow</i>
36	9.823E-5	1.9361E-8	0.925219
37	9.823E-5	2.1399E-8	0.977799
38	1.0857E-4	1.9361E-8	0.923916
39	1.0857E-4	2.1399E-8	0.925219

Table 23. Run of a 5% Design Centered on 9th Step

Four axial points were added at $\pm\alpha$ along each of the two axes to develop a central composite design. α was chosen to equal the fourth root of the number of factorial points in the full factorial design, 1.414 in this case, as suggested by Auclair (5). The additional axial points are shown in Table 24.

<i>Run No.</i>	<i>Transmissivity</i>	<i>Discharge</i>	<i>RMS flow</i>
40	1.1071E-4	2.038E-8	0.919488
41	9.60885E-5	2.038E-8	0.958185
42	1.034E-4	2.1821E-8	0.954969
43	1.034E-4	1.8939E-8	0.919911

Table 24. Additional Points Centered on 9th Step

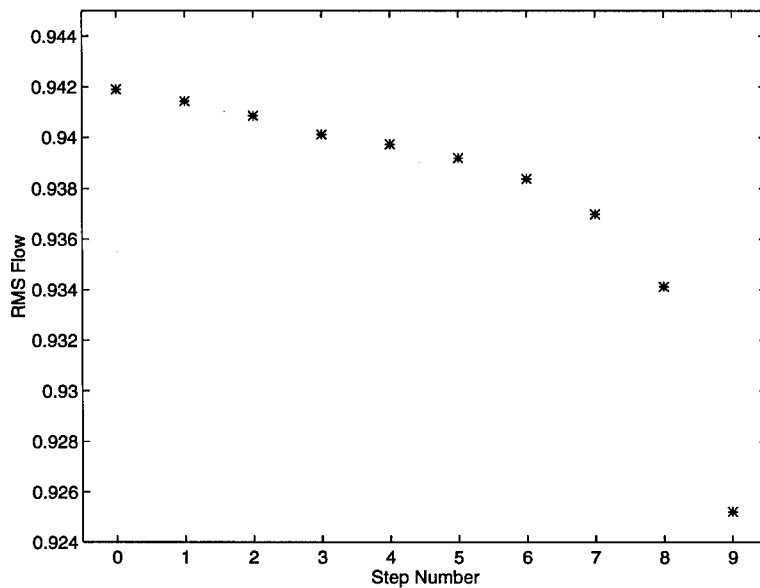


Figure 5. Graph of RMS Flow Along Second Gradient Vector

All nine points in the design on the 9th step were then run through a second order model in SAS. This model approximated the coefficients of equation 21; the SAS results are shown in Appendix C-7 and include a canonical and a ridge analysis.

$$Y = \beta_0 + \beta_T T + \beta_D D + \beta_{TT} T^2 + \beta_{DD} D^2 + \beta_{TD} TD \quad (19)$$

The canonical analysis shows a local minimum could exist at a transmissivity value of -0.595968 (1.00319E-4 uncoded) and a discharge value of -1.689911 (1.8658E-8 uncoded). This point was run through Bioplume for an RMS flow value of 0.918963 feet.

The ridge analysis used SAS to extrapolate out from the design region to find points that would be good candidates for further exploration. The results of the ridge analysis are shown in Appendix C-7. Four points along the predicted ridge were tested to see if a ridge of decreasing response really existed and if the responses were better than at the stationary point predicted by the canonical analysis. See Table 25 for results of the ridge analysis. Note that the distance along the ridge given in the table is in coded units.

Run No.	Distance along Ridge	Transmissivity (coded)	Discharge (coded)	RMS flow
44	1	1.03696E-4 (0.057195)	2.13973E-8 (-0.998363)	0.942336
45	2	9.95182E-5 (-0.750829)	1.84911 (-1.853714)	0.918993
46	3	9.5795E-5 (-1.470982)	1.77157 (-2.614615)	0.919196
47	4	9.2159E-5 (-2.174265)	1.69587 (-3.357465)	0.919517

Table 25. Ridge Analysis for RSM Flow Calibration

Because the ridge analysis did not improve the response beyond the value of the stationary point the calibration was stopped. The best response found during the ridge analysis was 0.918993 feet at a transmissivity of 9.95182E-5 square feet/second and a discharge of 1.84911 feet/second.

The best response found was not actually at the stationary point, but at the corner of the second of the first order designs. This value occurred at a transmissivity of 1.53E-3 square feet per second and a discharge of 2.86E-7 feet per second. The root mean squared error criterion at this point was 0.918875 feet, which was less than a ten thousandth of a foot lower in response than the stationary point. If RSM had been halted at this point, then a superior response would have been obtained using RSM in only 24 runs of the Bioplume-II model. The RSM calibration was not terminated, however, because in exploring the capabilities of the procedure the specific response at run number 24 was simply overlooked.

4.2.4.2 RSM Transport Calibration. For the transport calibration five factors had to be considered. These were longitudinal dispersivity (α_L), the ratio of transverse to longitudinal dispersivity ($\frac{\alpha_T}{\alpha_L}$), the stoichiometric ratio (F), the retardation factor (R_f), and the Reaeration Coefficient (RC).

Screening Phase of RSM Transport Calibration. Using a full factorial design, a screening phase was run for all the factors. This design included $2^5 = 32$ runs at the high and a low levels for each factor. These levels are shown in Table 26, and the results of these runs are given in the SAS output in Appendix C-8.

Factor	Low	High
α_L	32.8	137.46
$\frac{\alpha_T}{\alpha_L}$	0.001	1.0
F (Stoichiometric Coefficient)	2.0	4.0
$K_D (R_f)$	0 (1.00)	0.11299 (1.40)
Reaeration Coefficient	0	0.005

Table 26. Details of Screening Design Levels

Although the screening design suggested that the stoichiometric ratio and the retardation factor had the least effect on the response, the response surface required special treatment. Two of the 32 runs had response values below the 67.1831 that resulted from most of the One-Factor calibration approach. These values were obtained only when the stoichiometric ratio was set to a high value and the Reaeration coefficient was set to zero (uncoded).

Only two factors were considered for further calibration, the longitudinal dispersivity and the ratio of transverse to longitudinal dispersivity. The stoichiometric ratio and the reaeration coefficient were set to their high and low values respectively. Because of its apparently minimal impact on response, the retardation factor was set to the one, i.e. no retardation.

First-Order Phase of RSM Transport Calibration. The starting location selected for the first-order design coincided with the lowest response observed in the screening phase. This point could not be used as the center of a new design, however, because it was on the boundary of reasonable values of the parameters. Therefore, an arbitrary design was chosen that included the minimum point as a corner. This choice meant setting the stochastic ratio to 4.0 (+1 coded) and the reaeration coefficient to zero. The retardation factor was set to zero (-1 coded) because this value led to the lowest response in the screening design. The remaining two factors were then varied and the results were as shown in Table 27.

These responses were then fit to a first-order regression model using SAS. The output is shown in Appendix C-9. These results show that a very poor fit was obtained.

run No.	α_L	$\frac{\alpha_T}{\alpha_L}$	RMS Transport
33	123.714	0.001	67.1906
34	123.714	0.002	67.0921
35	137.46	0.001	67.0505
36	137.46	0.002	67.1115

Table 27. First-Order Design for RSM Transport Calibration

Second-Order Phase of RSM Transport Calibration.

A second-order design was next used to improve the calibration. Additional tests were made at 1.414 coded units away from the design center along each axis. These coordinates would have rendered some tests out of the feasible range of factor values. To avoid this problem, the readings were taken at one coded unit along the axis when necessary. A face centered central composite design would have been a more conventional choice for this design, but this unusual design worked acceptably well. The center of the design was also included for a total of five additional points. The results are shown in Table 28.

Run No.	α_L (coded)	$\frac{\alpha_T}{\alpha_L}$ (coded)	RMS Transport
37	120.869 ($-\sqrt{2}$)	0.0015 (0)	67.2464
38	137.46 (+1)	0.0015 (0)	67.0764
39	130.587 (0)	0.002207 ($+\sqrt{2}$)	67.0327
40	130.587 (0)	0.001 (-1)	67.0394
41	130.587 (0)	0.0015 (0)	67.0362

Table 28. Second-Order Design for RSM Transport Calibration

A ridge analysis was performed using the nine data points tested. The SAS output is shown in Appendix C-10. The analysis predicted a ridge pointing in the direction of decreasing longitudinal dispersivity and increasing transverse dispersivity. First the stationary point identified by the canonical analysis was tested and then points were tested along the predicted location of the ridge. As shown in Table 29, no change in response was identified.

Run No.	units along ridge	α_L (coded)	$\frac{\alpha_T}{\alpha_L}$ (coded)	RMS Transport
42	Stationary Point	131.66 (0.155432)	0.00161 (0.220709)	67.1831
43	1	129.92 (-0.096925)	0.0021 (1.200923)	67.1831
44	2	128.27 (-0.336868)	0.0026 (2.202779)	67.1831
45	3	126.65 (-0.572427)	0.0031 (3.184661)	67.1831
46	4	125.041 (-0.806931)	0.0036 (4.161754)	67.1831
47	5	123.43 (-1.041017)	0.0041 (5.136951)	67.1831

Table 29. Ridge Analysis for RSM Transport Calibration

At this point the calibration was stopped due to the lack of sufficient improvement in the response. The RSM transport phase took 47 runs and had a best response of 67.0327 parts per billion, identified at $\alpha_L = 130.587$ and $\frac{\alpha_T}{\alpha_L} = 0.002207$.

4.3 Summary

Table 30 summarizes the results of the two calibrations to allow for a comparison. It can be seen that RSM took longer to converge, but always led to better results.

Method	Best Result	Total Runs	Expected Runs
Flow Calibration			
One-Factor	0.921225	36	
RSM	0.918875	47	24-43
Transport Calibration			
One-Factor	67.1831	21	
RSM	67.0327	47	23

Table 30. Summary of Calibrations

Note the "Expected Runs" column lists the number of runs that would have been required if efficient Plackett-Burman or Fractional Factorial designs had been used for the Screening design. The range shown for RSM flow calibration (24-43 runs) reflects the fact that the best value for this calibration was obtained on the 24th run. Since all runs after that were not as good, the calibration could have been reasonably stopped at any time after that run.

The fact that RSM took more runs than the one-factor-at-a-time approach in the flow calibration may be partially because RSM was used in an exploratory manner. If the RSM flow calibration had been halted when it surpassed the one-factor-at-a-time approach, only 19 runs would have been required with efficient Plackett-Burman or Fractional Factorial Screening designs.

The comparison for the transport calibration does not present the full picture either. The one-factor-at-a-time approach made no progress at all. To take the time to find the a response of 67.0327 feet using the one-factor-at-a-time approach would most likely have taken many more runs than the RSM technique took. By finding an area of improved response on the transport surface, RSM performed better than the one-factor-at-a-time approach.

V. Conclusions and Recommendations

5.1 Conclusions

The results were not impressive for either technique. This was likely caused by the use of the homogeneity assumption for all environmental factors calibrated. The MADE-2 site is well known in the literature for its heterogeneity (50). This difference between the simulated and actual conditions could prevent significant improvement in response regardless of calibration technique.

The strength of RSM could have become more apparent if zonation had been used. A zonated model would allow for significant improvement in response, but would have added significantly to the number of factors involved in the calibration. The one-factor-at-a-time approach would have been tedious to use for a zonated model. RSM would excel here due to the use of the Screening phase and the application of efficient Plackett-Burman or Fractional Factorial designs. RSM would save runs by calibrating only the most significant factors.

The major weakness of the one-factor-at-a-time approach demonstrated by this research was its inability to take interactions between parameters into consideration during the calibration process. By varying one parameter at a time the method used a tunnel vision approach. In effect, the approach can only turn at right angles while negotiating a response surface. RSM improves on this approach by simultaneously varying every parameter to improve the response. This gradient search approach allows RSM users to obtain a better sense of the response surface and move in any direction to improve the response.

One difficulty with the use of RSM is that the modeler must have knowledge of some statistical concepts beyond those of many engineers and hydrogeologists. A solution to this problem is that when the modeler is not familiar with the material, another individual in the organization possibly could be assigned to assist with the calibration. If this is not the case, specialized training may be needed to enable modelers to use this approach.

Another problem with the use of RSM is that a statistical software package may be needed to take full advantage of the second-order techniques. Not every environmental engineering organization has access to this type of software. However, the first-order and some of the second-order techniques may be used with a spreadsheet or even a calculator. They still have the advantage of varying more than one factor at a time and therefore take interactions between parameters into consideration. Therefore, lack of access to an advanced statistical software package does not limit the modeler to the one-factor-at-a-time approach.

RSM took longer to find the best response identified than the one-factor-at-a-time approach. This was partly the result of the researcher's inexperience with the method. RSM also took longer because it was not used in the most efficient way possible. Full factorial designs were used all the way through the research because of their simplicity. If Plackett-Burman or other fractional factorial designs had been used the number of runs would have been reduced significantly.

RSM showed a strength in the calibration of the transport phase. The one-factor-at-a-time approach was unable to make any progress after varying all five transport parameters throughout a feasible range. In order to continue the calibration using this approach, a new starting point would be selected and the parameters again varied. The problem is that the areas of improved response were not easy to find. The traditional method would have difficulty improving upon model response in this case. Without a systematic procedure to vary one parameter with respect to the others, one-factor-at-a-time calibration is little more than iterative guessing.

The greatest strength of RSM is in its ability to move over the response surface while taking interactions between parameters into account. This strength allowed it to find a region of improved response. In the transport case the improvement was roughly 0.1 ppb. Although this improvement is small, it is real because the model is deterministic. The region was probably a narrow and shallow depression in the transport calibration error response surface, but it would be difficult to find at all without a systematic procedure. RSM found it easily by

varying all the parameters simultaneously. If only one factor is varied at a time, many features of the response surface will not be identified.

5.2 *Recommendations*

For further research in this area the following are recommended:

1. Reduce the simulated time from 15 months to a few months in order to avoid the problem created by the plume disappearing in the simulation. This change should reduce the prevalence of the 67.1831 response for the transport calibration and improve the behavior of the transport response surface.
2. Zonate some of the parameters to increase model accuracy. Zonation of parameters such as transmissivity and dispersivity might significantly improve model response and drop the average error response. This change would also show the strength of RSM in its ability to vary large numbers of parameters while exploring the response surface.
3. Repeat the exercise on another data set or using another model. This repetition might provide an indication of how RSM compares to the one-factor-at-a-time approach overall, rather than just for Bioplume II using MADE-2 data, as in this research.
4. Calibrate both flow and transport simultaneously by using the sum of the RMS flow and transport criteria for the error response surface. This approach could improve calibration by taking interactions between degree of flow calibration and transport calibration into account.
5. Repeat the research using fractional factorial designs to see how far the number of required runs could be reduced.
6. Repeat the research using several different error criteria to compare their effect on convergence.
7. Repeat the research using transient hydraulics to see whether the success of each calibration technique depends on that aspect of the modeling.

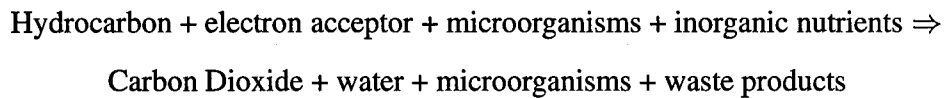
Appendix A. Biodegradation of Petroleum Hydrocarbons

The contamination of soil and groundwater has become a major issue in the media over the past 20 years. The result of the public's interest in the issue was the passage of laws such as the Comprehensive Environmental Response, Compensation and Liability Act (CERCLA) requiring cleanup of contaminated sites. The U.S. Air Force necessarily has interest in the issue due to the number of contaminated sites located on Air Force (AF) bases. The extensive use of jet fuels by the AF has led to a special interest in the remediation of petroleum hydrocarbons in the subsurface. Due to the high solubility of some aromatic hydrocarbons, such as benzene, toluene, ethylbenzene, and xylenes (BTEX), they pose an extra risk to human health and the environment. This appendix will therefore focus on aromatic hydrocarbons.

Of all the remediation technologies, natural attenuation stands out as holding unusual potential to decrease the cost of remediating many contaminated sites. Natural attenuation is a remedial action where subsurface microorganisms, in combination with geophysical factors, naturally clean the soil and groundwater. The potential savings are huge.

The natural attenuation process involves four factors: volatilization, dispersion, sorption and degradation. Volatilization is the transfer of contamination from aqueous to vapor phases. Dispersion is the spreading out of contaminants that reduces concentration, but not total mass. Sorption is the adsorption of contaminants to the soil matrix. This process reduces concentration of contaminants in groundwater, but not total mass. Degradation includes both abiotic chemical and biotic transformation of contaminant species into other substances. This process reduces the concentration and mass of contaminant. McAllister and Chiang (38:163-164) notes that biodegradation is usually the most significant degradation process in the subsurface. Stauffer and others (51:78) supported this conclusion by showing that the effect of sorption on plume stabilization was negligible compared to the effect of biodegradation at a site under aerobic conditions.

The concept of biodegradation of petroleum hydrocarbons is that the microorganisms use the contaminant as a food source. The general equation can be seen as (11:179):



Biodegradation is classified as aerobic if the electron acceptor is molecular oxygen and anaerobic otherwise. Liss and Baker (36:303) list nitrate, sulfate, carbonate, iron and manganese oxide as alternative electron acceptors. Aerobic biodegradation requires at least 1-2 ppm dissolved oxygen and can rapidly degrade some compounds. First order rate constants of 0.3-1.3/

The rate of biodegradation may be measured using the Respiration Quotient (30:477) equal to actual respiration over potential respiration, where potential respiration was microbial oxygen uptake measured after addition of an easily biodegradable carbon source, such as glucose. They found a correlation coefficient of 0.997 between the quotient and concentration of polycyclic aromatic hydrocarbons (PAH) showing the respiration coefficient was an indicator of microbial metabolic activity.

Leahy and Colwell (35:307) note the impact of physical factors on microbial activity. They cite research by Atlas and Bartha observing that low temperatures inhibit microbial activity and research by Bossert and Bartha observing that higher temperatures increase activity up to a point, beyond which disruption occurs. They also cite Dibble and Bartha in concluding that extremely high concentrations of petroleum hydrocarbons may decrease activity due to toxicity effects of components in the petroleum mixture.

It is clear that some toxicity could occur because of the wide variety of compounds present in the petroleum hydrocarbon mixture. Atlas and Bartha (4:393-394) explain that a typical petroleum mixture includes aliphatics, alicyclics, aromatics and other organics.

The microorganisms that metabolize hydrocarbons are mostly bacteria and fungi (35:308). Rainwater and Scholze (43:108) cite a study by Ghiorse and Balkwill which approximated the number of bacteria in the subsurface at one million per gram of dry soil. Chapelle (18:336) notes that *Pseudomonas putida* has been shown in studies by Gibson and others at the University of Texas to be capable of degrading benzene, toluene and ethylbenzene.

Leahy and Colwell (35:308) listed *Archromobacter*, *Acinetobacter*, *Alcaligenes*, *Arthrobacter*, *Bacillus*, *Flavobacterium*, *Nocardia* and *Pseudomonas* as the most important hydrocarbon degrading bacterial genera. They list *Trichoderma*, *Mortierella*, *Asperigillus* and *Penicillium* as the most important fungal genera in soil media. Other genera noted in the literature for their hydrocarbon degrading ability include *Xanthobacter* (54:1287) and *Desulfobacterium* (8:178). Bak and Widel isolated a new species, *Desulfobacterium phenolicolum*, an obligatory anaerobic halophile, capable of metabolizing phenol. Szewzyk and Pfennig (53:164-165) identified *Desulfobacterium catecholicum*, a strictly anaerobic, sulfate reducing bacterium, capable of chemolithoautotrophic growth on hydrogen and carbon dioxide or heterotrophic growth on organics such as catechol. Heitkamp and Cerniglia (29:1612) isolated a halotolerant strain capable of mineralizing naphthalene, phenanthrene, fluoranthrene, pyrene and other aromatics to carbon dioxide when supplied with nutrients in the laboratory. Cutright and Lee (22:404) identified a species of *Mycobacterium* capable of metabolizing polycyclic aromatic hydrocarbons.

Although protozoans do not appear to utilize hydrocarbons directly (35:309), Madsen and others (37:252) observed high density protozoan populations growing in a hydrocarbon plume. The protozoans prey on bacteria that metabolize the hydrocarbons. They noted that elevated protozoan biomass acts as an indicator of the biodegradation activity.

After a petroleum hydrocarbon is introduced to a microbial population there will typically be a lag time before biodegradation begins (58:1000) (28:256). During this period the microbial population may be adapting to the petroleum hydrocarbon. Leahy and Colwell (35:309) define adaptation as the effect of prior exposure in determining the rate at which a microbial community will biodegrade hydrocarbons and cite Spain and others in defining three mechanisms of adaptation: (1) changes in the action of enzymes, (2) mutations to genes allowing new metabolic pathways and (3) natural selection for organisms with the metabolic capability to degrade the petroleum hydrocarbon. They note that DNA encoded on plasmid may play an important role in genetic adaptation for hydrocarbon metabolism because of its high mobility due to conjugation and transformation. They cited a study by Chakrabarty on

Pseudomonas that showed plasmid DNA was encoded for metabolism of xylene, toluene, naphthalene and other compounds suggesting it may play a strong role in adaptation.

Zeyer and others (65:946) demonstrated cross-acclimation, defined as exposure to one compound increasing the metabolism of other compounds of similar structure (35:309), by demonstrating microorganisms adapted to m-xylene had a shorter lag time than expected when metabolizing toluene.

Some authors report no adaptation. Angley and others (3:1406) observed no lag period in lab experiments on aerobic degradation of BTEX compounds and other alkylbenzenes. Davis and others (23:221) observed no lag time in experiments on aerobic degradation of benzene until initial benzene concentration was increased from about 1 ppm to 10 ppm. After the increase a 10 day lag occurred before biodegradation began. The absence of a lag period indicates the microorganisms have no need to adapt to the substrate before they can begin metabolism.

The rate at which metabolism occurs may be influenced by the molecular structure of the hydrocarbon. Leahy and Colwell (35:305) cite Perry who ranks petroleum compounds in decreasing order of susceptibility to biodegradation: n-alkanes, branched alkanes, low molecular weight aromatics, and cyclic alkanes. Chapelle (18:350) cites a study by Barker and others where benzene, toluene and xylenes were injected into an aquifer. They found relative degradation rates under aerobic conditions to be: xylenes > toluene > benzene. Under anaerobic conditions toluene and the xylenes were almost gone by 108 days. Benzene was almost gone by 400 days.

Stauffer and others (51:73) supported the work of Barker and others noted above. They injected contaminants into groundwater with a tritiated water tracer and monitored contaminant concentrations. They verified p-xylene degrades faster than benzene under aerobic conditions (51:82) . Their results showed rapid BTEX biodegradation under aerobic conditions.

Angley and others (3:1406) performed lab experiments on aerobic degradation with BTEX compounds and other alkylbenzenes, demonstrating a decrease in concentration to

below detection limits (a decrease of four orders of magnitude for the BTEX compounds) within 31 days. This was accompanied by rapid decreases in dissolved oxygen concentration.

Davis and others (23:221) studied biodegradation in the lab. They showed a decrease in benzene concentration of 50% (from about 1 ppm) after four days under aerobic conditions. The biologically-inhibited controls, on the other hand, showed only 2-18% concentration decreases. When initial benzene was increased to about 10 ppm, 50% of the benzene was gone after 14 days with complete degradation by 35 days. Under sulfate reducing anaerobic conditions, 77 days were required to degrade 90% of 1 ppm benzene.

Morgan and others (40:189) studied both aerobic and anaerobic degradation in the lab. They found that under aerobic conditions BTEX rapidly biodegraded. Furthermore they found oxygen supply to be the limiting factor for degradation, and found that no biodegradation occurred under anaerobic conditions, unless nitrate was added as an electron acceptor.

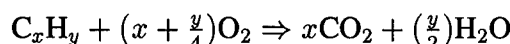
Baedecker and others (6:569) studied samples from a site in Minnesota under anaerobic conditions. Their data showed benzene and alkylbenzenes degrade under aerobic conditions. 98% degradation of benzene and toluene occurred in 125 and 45 days respectively. This was coupled with increases in iron and manganese concentrations, suggesting metal reducing conditions.

Neilsen and others (41:461) performed a laboratory experiment on groundwater and mixed groundwater/sediment media. They found no degradation of benzene, toluene, or o-xylene under anaerobic conditions, but all were degraded under aerobic conditions. Degradation of benzene and toluene required 40 to 70 days and resulted in reduction to less than 10% of initial concentrations (41:465).

Other authors who have studied this subject include Wilson and others (59:61) whose lab studies confirmed field observations that aerobic and anaerobic biodegradation of alkylbenzenes occurred. Zeyer and others (65:944) showed complete mineralization of toluene and m-xylene under anoxic denitrifying conditions using a continuous flow system. Wilson and

others (58:997) demonstrated methane fermentation (anaerobic biodegradation) of toluene in an aquifer.

The process of biodegradation is one of enzymatic transformation through a series of metabolic intermediate stages. In the case of mineralization the end products are carbon dioxide and water. Kerfoot (33:877) gave a simplified form of the stoichiometric equation for aerobic biodegradation:



For benzene, the degradation process involves, first, transformation to a catechol intermediate and then breakdown of the ring structure through ortho or meta cleavage. Oxidation of benzene via the enzyme benzene dioxygenase to form cis-benzene dihydrodiol is the first step. The second step involves hydrogen removal via the enzyme nicotine adenine dinucleotide (NAD). A diagram of this process is shown in Figure 6.

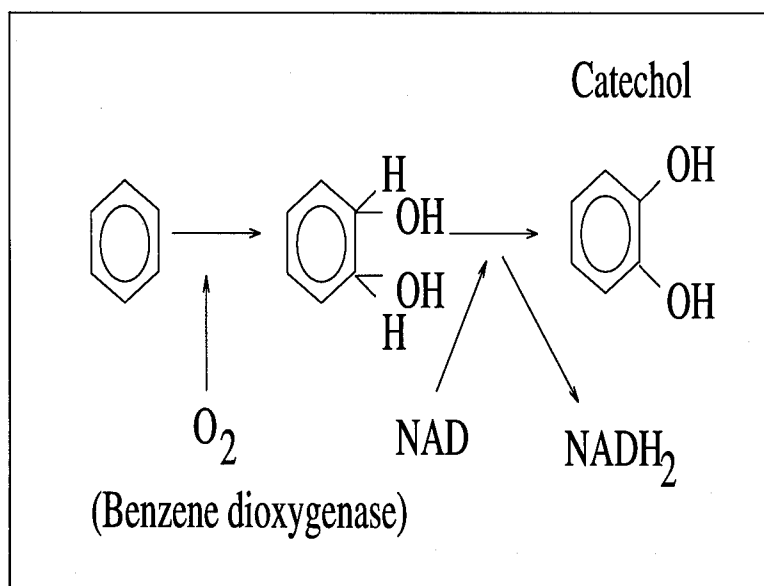


Figure 6. Biodegradation of Benzene to Catechol
(18:337)

The ortho cleavage of catechol involves breaking the ring structure between the two hydroxyl groups. Chapelle (18:338) describes the ortho cleavage pathway through several steps. A diagram is shown in Figure 7.

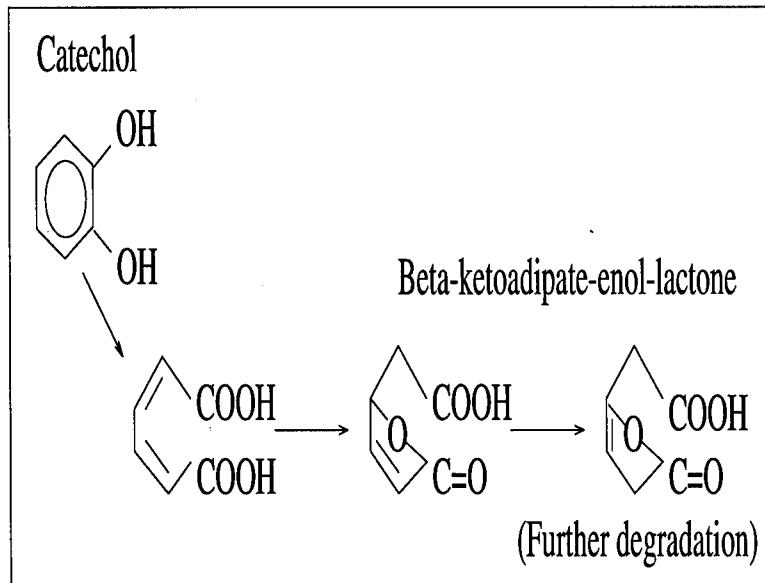


Figure 7. Ortho-Cleavage Pathway
(18:338)

The alternative meta cleavage pathway involves ring breakage beside one of the two hydroxyl groups on the catechol, followed by insertion of two oxygen atoms via the enzyme catechol 2,3-dioxygenase. The ring is then cleaved by a hydrolase (water removing enzyme). Further degradation of the organic acid product to CO_2 may then occur. A diagram is shown in Figure 8. Note that beta-oxidation in the figure refers to oxidation of the middle carbon and removal as carbon dioxide.

Chapelle (18:337) notes that ortho and meta cleavage of catechol has been identified in *Pseudomonas putida*, *Acinetobacter*, *Bacillus*, *Alcaligenes* and *Nocardia*. Breakdown of toluene and xylenes via *Pseudomonas* follow processes similar to that of benzene except that toluene and xylenes form methyl- and dimethylcatechol respectively, and both follow the meta-cleavage pathway (18:339).

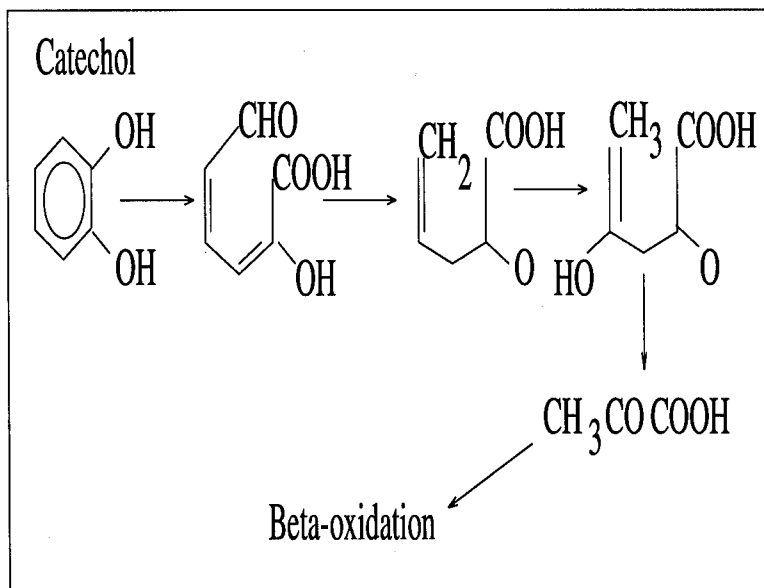


Figure 8. Meta-Cleavage Pathway
(18:338)

Anaerobic transformation of benzene and toluene was studied, using gas chromatography/mass spectrometry (28:254). Results suggest initial ring hydroxylation or methyl-oxidation (in the toluene case) leading to phenol, cresol and aromatic alcohol intermediates. They observed incomplete mineralization to methane and carbon dioxide. Cozzarelli and others (20:138-140) support these findings. They identified oxygenated intermediates resulting from anaerobic degradation. Benzene produced phenol, toluene produced benzoic acid and xylenes produced toluic acids. The theoretical degradation pathways are shown in Figures 9 and 10.

Cozzarelli and others (21:863) found that benzene and alkylbenzenes degrade to organic acid intermediates under anaerobic conditions. They also found that reduction of iron, manganese, and nitrogen accompanied oxidation of the aromatics. Anaerobic biodegradation by denitrification is insignificant under natural conditions due to the usually low levels of nitrate in most contaminated aquifers (18:344).

Benzene degradation under methanogenic conditions begins with oxidation of benzene to phenol, through several aliphatic acids to final production of carbon dioxide and methane

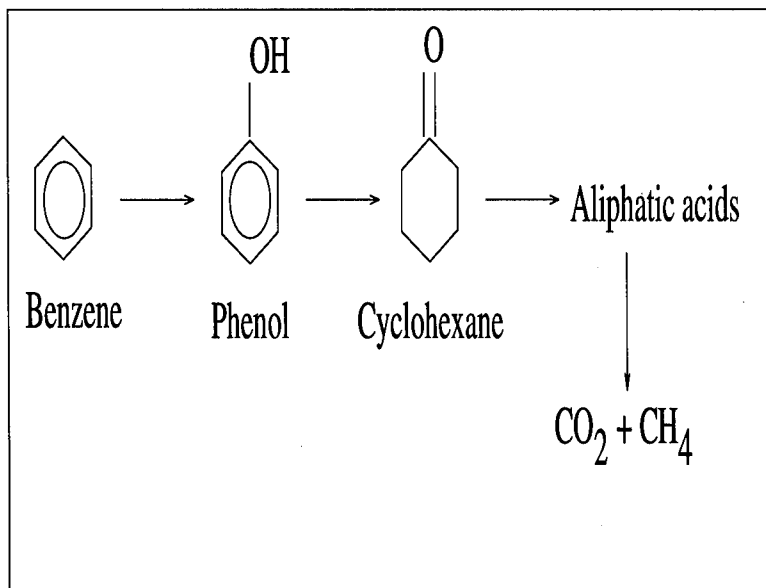
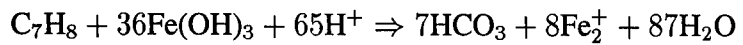


Figure 9. Anaerobic, Ring Hydroxylation of Benzene
(28:258)

(18:341). Degradation of toluene under methanogenic conditions begins with oxidation to benzylalcohol and then to benzaldehyde, benzoic acid, and through several aliphatic acid stages to become carbon dioxide and methane. Cozzarelli and others (20:138-140) may support this through their study of a site in Minnesota. Under anaerobic conditions, they monitored benzene transformation to phenol and toluene transformation to benzoic acid. Alternatively toluene may oxidize directly to ortho or p-cresol and then to carbon dioxide and methane (18:341).

Under iron reducing conditions degradation of toluene is to benzylalcohol, benzaldehyde, benzoate, and finally to carbon dioxide. At each step oxidation of the aromatic is accompanied by reduction of Fe(III) to Fe(II) (18:343). Baedecker and others (6:580) show a theoretical stoichiometric equation for transformation of toluene using Iron (III) Hydroxide as an electron acceptor:



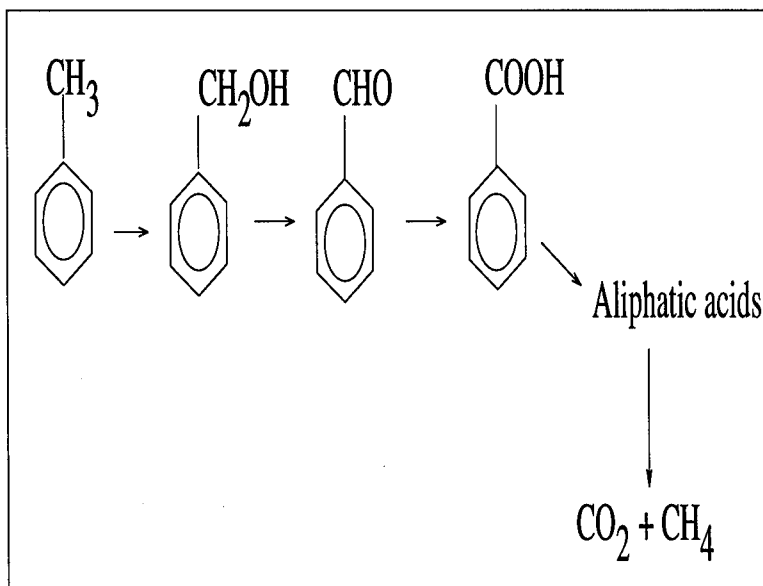


Figure 10. Anaerobic, Methyl-Oxidation of Toluene
(28:258)

The oxygen from the iron (III) hydroxide was inserted into the ring structure of toluene in this example. In other anaerobic cases the source of oxygen inserted into ring structures may be the water itself. Vogel and Grbic-Galic (55:200) used ^{18}O -labeled water to show that for the first oxidation step in the anaerobic transformation of benzene and toluene under methanogenic conditions, the oxygen atom came from water.

Clearly, a variety of microbial genera are capable of metabolizing many aromatic petroleum hydrocarbon compounds. Many conditions once thought prohibitive of biodegradation are now proven possibilities for natural attenuation. Although the data suggest aerobic biodegradation may occur more rapidly than anaerobic biodegradation, it is apparent that both may effectively reduce BTEX concentrations in an aquifer. If this approach received more regulatory acceptance, savings of restoration dollars are possible. Remedial costs for natural attenuation candidate sites could be significantly lower than under alternative technologies. If natural systems can be self-cleaning, public funds could be used somewhere other than on IRP sites.

Appendix B. Initial Bioplume Input File

Bioplume Input File for MADE-2 data

0.0 203.8 203.8 203.8 203.7 203.7 203.7 203.7 203.8 203.8 203.7 203.7 203.7 203.7 203.7 203.7 203.7 203.8 203.9 203.9 0.0
 0.0 203.9 203.8 203.8 203.8 203.8 203.8 203.8 203.8 203.8 203.8 203.7 203.7 203.7 203.6 203.6 203.7 203.8 203.9 203.9 0.0
 0.0 203.9 203.9 203.9 203.9 203.9 203.8 203.9 203.9 203.9 203.8 203.8 203.7 203.7 203.7 203.7 203.8 203.9 203.9 203.9 0.0
 0.0 204.0 204.0 203.9 203.9 203.9 203.9 203.9 203.9 203.9 203.8 203.7 203.7 203.7 203.7 203.7 203.8 203.9 204.0 204.0 0.0
 0.0 204.0 204.0 204.0 204.0 204.0 204.0 204.0 204.0 204.0 204.0 203.9 203.8 203.8 203.7 203.7 203.7 203.8 203.9 204.0 204.0 0.0
 0.0 204.1 204.1 204.1 204.1 204.1 204.1 204.1 204.1 204.1 204.0 204.0 204.0 204.0 204.0 204.0 203.9 203.8 204.0 204.1 0.0
 0.0 204.2 204.2 204.2 204.2 204.2 204.2 204.2 204.2 204.2 204.1 204.1 204.1 204.0 204.0 204.0 203.9 203.8 204.0 204.1 0.0
 0.0 204.2 204.2 204.2 204.2 204.3 204.3 204.3 204.3 204.3 204.3 204.3 204.2 204.2 204.2 204.1 204.0 204.1 204.1 204.2 0.0
 0.0 204.3 204.3 204.3 204.3 204.4 204.4 204.4 204.4 204.4 204.4 204.4 204.3 204.3 204.2 204.2 204.2 204.2 204.3 204.3 0.0
 0.0 204.3 204.3 204.4 204.4 204.4 204.4 204.5 204.5 204.5 204.5 204.6 204.6 204.5 204.5 204.4 204.4 204.4 204.4 204.4 0.0
 0.0 204.4 204.4 204.4 204.5 204.5 204.5 204.5 204.6 204.6 204.6 204.8 204.8 204.6 204.6 204.5 204.5 204.5 204.5 204.5 0.0
 0.0 204.4 204.5 204.5 204.5 204.6 204.6 204.6 204.7 204.7 204.8 204.8 204.7 204.7 204.6 204.6 204.6 204.6 204.6 204.6 0.0
 0.0 204.5 204.5 204.6 204.6 204.6 204.7 204.7 204.8 204.8 204.9 204.8 204.8 204.8 204.7 204.7 204.7 204.8 204.8 204.7 204.7 0.0
 0.0
 0.0
 1 1000.
 0.00
 0.00 5.37 5.41 5.44 5.48 5.50 5.52 5.53 5.50 5.42 5.24 4.82 4.12 3.36 3.11 3.16 3.24 3.31 3.38 0.00
 0.00 5.35 5.39 5.43 5.47 5.50 5.52 5.53 5.50 5.43 5.27 4.85 4.08 3.30 3.06 3.14 3.22 3.31 3.38 0.00
 0.00 5.33 5.37 5.41 5.45 5.48 5.51 5.52 5.49 5.41 5.26 4.92 4.07 3.44 3.18 3.19 3.26 3.34 3.41 0.00
 0.00 5.30 5.34 5.38 5.42 5.45 5.48 5.49 5.47 5.37 5.12 4.62 3.98 3.54 3.32 3.29 3.33 3.40 3.46 0.00
 0.00 5.26 5.30 5.34 5.38 5.41 5.44 5.46 5.44 5.33 4.96 4.20 3.84 3.61 3.46 3.41 3.44 3.48 3.53 0.00
 0.00 5.22 5.26 5.29 5.33 5.36 5.39 5.41 5.40 5.34 5.00 4.13 3.85 3.70 3.59 3.55 3.56 3.59 3.62 0.00
 0.00 5.17 5.20 5.24 5.27 5.30 5.32 5.33 5.33 5.32 5.17 4.39 4.00 3.83 3.74 3.70 3.69 3.71 3.73 0.00
 0.00 5.11 5.15 5.18 5.20 5.23 5.24 5.24 5.22 5.17 4.96 4.49 4.15 3.98 3.89 3.85 3.84 3.83 3.84 0.00
 0.00 5.06 5.08 5.11 5.13 5.14 5.15 5.13 5.08 4.98 4.78 4.49 4.26 4.12 4.05 4.01 3.99 3.97 3.96 0.00
 0.00 4.99 5.01 5.04 5.05 5.06 5.05 5.02 4.95 4.81 4.61 4.46 4.33 4.25 4.20 4.17 4.14 4.11 4.08 0.00
 0.00 4.92 4.94 4.96 4.97 4.97 4.96 4.92 4.83 4.68 4.46 4.44 4.41 4.38 4.36 4.33 4.30 4.25 4.20 0.00
 0.00 4.85 4.87 4.88 4.89 4.89 4.87 4.83 4.75 4.62 4.49 4.48 4.50 4.51 4.51 4.49 4.46 4.40 4.33 0.00
 0.00 4.78 4.79 4.80 4.80 4.80 4.79 4.76 4.70 4.61 4.54 4.55 4.60 4.64 4.67 4.66 4.61 4.53 4.44 0.00
 0.00 4.70 4.71 4.72 4.72 4.72 4.70 4.67 4.62 4.59 4.64 4.71 4.78 4.82 4.83 4.77 4.66 4.54 0.00
 0.00 4.62 4.63 4.63 4.63 4.64 4.64 4.64 4.64 4.62 4.73 4.82 4.89 4.96 4.99 4.91 4.77 4.63 0.00
 0.00 4.54 4.54 4.54 4.55 4.55 4.57 4.59 4.62 4.67 4.74 4.86 4.91 4.98 5.08 5.15 5.03 4.85 4.68 0.00
 0.00 4.46 4.45 4.45 4.45 4.46 4.48 4.52 4.59 4.69 4.85 4.97 4.95 5.00 5.12 5.28 5.08 4.88 4.70 0.00
 0.00 4.38 4.36 4.36 4.35 4.36 4.38 4.43 4.52 4.66 4.83 4.92 4.90 4.95 5.05 5.13 5.02 4.85 4.69 0.00
 0.00 4.29 4.27 4.26 4.25 4.25 4.27 4.32 4.42 4.57 4.70 4.73 4.76 4.82 4.90 4.95 4.90 4.78 4.64 0.00
 0.00 4.20 4.18 4.16 4.14 4.13 4.13 4.17 4.26 4.42 4.56 4.54 4.56 4.63 4.72 4.77 4.75 4.67 4.57 0.00
 0.00 4.12 4.09 4.06 4.03 4.00 3.98 3.99 4.03 4.19 4.41 4.25 4.31 4.41 4.51 4.58 4.59 4.55 4.48 0.00
 0.00 4.04 4.00 3.96 3.91 3.87 3.82 3.79 3.76 3.77 3.71 3.85 4.02 4.18 4.31 4.39 4.43 4.42 4.38 0.00
 0.00 3.96 3.91 3.86 3.80 3.74 3.67 3.59 3.48 3.31 3.19 3.49 3.76 3.96 4.12 4.22 4.28 4.29 4.28 0.00
 0.00 3.88 3.83 3.77 3.70 3.63 3.54 3.42 3.27 3.05 2.96 3.27 3.55 3.77 3.94 4.06 4.13 4.17 4.18 0.00
 0.00 3.81 3.75 3.69 3.61 3.53 3.43 3.30 3.15 2.99 2.97 3.17 3.41 3.62 3.79 3.92 4.00 4.05 4.08 0.00
 0.00 3.75 3.68 3.61 3.54 3.45 3.34 3.22 3.09 2.99 2.99 3.13 3.32 3.51 3.67 3.80 3.89 3.95 3.98 0.00
 0.00 3.69 3.62 3.55 3.47 3.38 3.28 3.18 3.07 3.00 3.01 3.11 3.27 3.43 3.58 3.70 3.79 3.85 3.90 0.00
 0.00 3.63 3.57 3.49 3.42 3.33 3.24 3.15 3.07 3.02 3.03 3.11 3.23 3.37 3.50 3.61 3.70 3.77 3.82 0.00
 0.00

Appendix C. SAS Output

C.1 Stepwise Procedure for RSM Screening Phase

SAS Program:

```
option linesize=80;
data d1;
  infile 'rsmphs1.dat';
  input t p d y;
  tp=t*p;
  td=t*d;
  pd=p*d;
  tpd=t*p*d;
proc print;
proc stepwise;
  model y = t p d tp td pd tpd/stepwise;
run;
```

SAS Output:

OBS	T	P	D	Y	TP	TD	PD	TPD
1	-1	-1	-1	27246.50	1	1	1	-1
2	-1	-1	1	544968.00	1	-1	-1	1
3	-1	1	-1	27246.50	-1	1	-1	1
4	-1	1	1	544968.00	-1	-1	1	-1
5	1	-1	-1	2.22	-1	-1	1	1
6	1	-1	1	1.81	-1	1	-1	-1
7	1	1	-1	2.22	1	-1	-1	-1
8	1	1	1	1.81	1	1	1	1

The SAS System 17
08:51 Friday, October 6, 1995

Stepwise Procedure for Dependent Variable Y

Step 1 Variable T Entered R-square = 0.37918514 C(p) = .

	DF	Sum of Squares	Mean Square	F	Prob>F
Regression	1	163712412173.29	163712412173.29	3.66	0.1041
Error	6	268035551562.41	44672591927.069		
Total	7	431747963735.70			

Variable	Parameter Estimate	Standard Error	Type II Sum of Squares	F	Prob>F
INTERCEP	143054.63198250	74726.66184759	163717021853.19	3.66	0.1041
T	-143052.6180175	74726.66184759	163712412173.29	3.66	0.1041

Bounds on condition number: 1, 1

The SAS System 18
08:51 Friday, October 6, 1995

Step 2 Variable TD Entered R-square = 0.68959305 C(p) = .

	DF	Sum of Squares	Mean Square	F	Prob>F
Regression	2	297730396829.23	148865198414.62	5.55	0.0537
Error	5	134017566906.47	26803513381.293		
Total	7	431747963735.70			

Variable	Parameter Estimate	Standard Error	Type II Sum of Squares	F	Prob>F
INTERCEP	143054.63198250	57882.97826358	163717021853.19	6.11	0.0564
T	-143052.6180175	57882.97826358	163712412173.29	6.11	0.0564
TD	-129430.4758625	57882.97826358	134017984655.95	5.00	0.0756

Bounds on condition number: 1, 4

The SAS System 19
08:51 Friday, October 6, 1995

Step 3 Variable D Entered R-square = 1.00000000 C(p) = .

DF	Sum of Squares	Mean Square	F	Prob>F

Regression	3	431747963735.70	143915987911.90	.	.
Error	4	0.00000000	0.00000000	.	.
Total	7	431747963735.70			

Variable	Parameter Estimate	Standard Error	Type II Sum of Squares	F	Prob>F
INTERCEP	143054.63198250	0.00000000	163717021853.19	.	.
T	-143052.6180175	0.00000000	163712412173.29	.	.
D	129430.27413750	0.00000000	134017566906.47	.	.
TD	-129430.4758625	0.00000000	134017984655.95	.	.

Bounds on condition number: 1, 9

All variables left in the model are significant at the 0.1500 level.
 No other variable met the 0.1500 significance level for entry into the model.

The SAS System 20
 08:51 Friday, October 6, 1995

Summary of Stepwise Procedure for Dependent Variable Y

Step	Variable Entered	Number Removed	Partial In	Model R**2	Model R**2	C(p)	F	Prob>F
1	T		1	0.3792	0.3792	.	3.6647	0.1041
2	TD		2	0.3104	0.6896	.	5.0000	0.0756
3	D		3	0.3104	1.0000	.	.	.

C.2 First Run of the First-Order Design Phase

SAS Program:

```
option linesize=80;
data d1;
  infile 'rsmphs2.dat';
  input t d y;
proc print;
proc reg;
  model y = t d;
run;
```

SAS Output:

The SAS System

7

08:51 Friday, October 6, 1995

OBS	T	D	Y
1	1	1	2.11605
2	1	-1	2.36023
3	-1	1	1.24133
4	-1	-1	3.37311

8

08:51 Friday, October 6, 1995

Model: MODEL1

Dependent Variable: Y

Analysis of Variance

Source	DF	Sum of Squares	Mean Square	F Value	Prob>F
Model	2	1.41607	0.70803	0.795	0.6214
Error	1	0.89076	0.89076		
C Total	3	2.30683			

Root MSE	0.94380	R-square	0.6139
Dep Mean	2.27268	Adj R-sq	-0.1584
C.V.	41.52806		

The SAS System

9

08:51 Friday, October 6, 1995

Parameter Estimates

Variable	Parameter DF	Estimate	Standard Error	T for H0: Parameter=0	Prob > T
----------	--------------	----------	----------------	-----------------------	-----------

INTERCEP	1	2.272680	0.47190000	4.816	0.1303
T	1	-0.034540	0.47190000	-0.073	0.9535
D	1	-0.593990	0.47190000	-1.259	0.4274

C.3 40% Design without Centerpoint

SAS Program:

```
option linesize=80;
data d1;
  infile 'rsmphs3.dat';
  input t d y;
proc print;
proc reg;
  model y = t d;
run;
```

SAS Output:

The SAS System 1
17:11 Thursday, October 26, 1995

OBS	T	D	Y
1	-1	-1	2.21077
2	-1	1	7.46751
3	1	-1	0.96785
4	1	1	2.21034

The SAS System 2
17:11 Thursday, October 26, 1995

Model: MODEL1

Dependent Variable: Y

Analysis of Variance

Source	DF	Sum of Squares	Mean Square	F Value	Prob>F
Model	2	21.12278	10.56139	2.622	0.4002
Error	1	4.02855	4.02855		

C Total 3 25.15133

Root MSE 2.00713 R-square 0.8398
Dep Mean 3.21412 Adj R-sq 0.5195
C.V. 62.44718

The SAS System

3

17:11 Thursday, October 26, 1995

Parameter Estimates

Variable	DF	Parameter Estimate	Standard Error	T for H0: Parameter=0	Prob > T
INTERCEP	1	3.214118	1.00356300	3.203	0.1927
T	1	-1.625022	1.00356300	-1.619	0.3522
D	1	1.624807	1.00356300	1.619	0.3522

C.4 40% Design With Centerpoint

SAS Program:

```
option linesize=80;
data d1;
  infile 'rsmphs3.dat';
  input t d y;
proc print;
proc reg;
  model y = t d;
run;
```

SAS Output:

The SAS System

21

08:51 Friday, October 6, 1995

OBS	T	D	Y
1	-1	-1	2.21077
2	-1	1	7.46751

3	1	-1	0.96785
4	1	1	2.21034
5	0	0	2.21077

The SAS System

22

08:51 Friday, October 6, 1995

Model: MODEL1

Dependent Variable: Y

Analysis of Variance

Source	DF	Sum of Squares	Mean Square	F Value	Prob>F
Model	2	21.12278	10.56139	4.370	0.1862
Error	2	4.83392	2.41696		
C Total	4	25.95670			
Root MSE		1.55466	R-square	0.8138	
Dep Mean		3.01345	Adj R-sq	0.6275	
C.V.		51.59065			

The SAS System

23

08:51 Friday, October 6, 1995

Parameter Estimates

Variable	DF	Parameter	Standard	T for H0:	Prob > T
		Estimate	Error	Parameter=0	
INTERCEP	1	3.013448	0.69526402	4.334	0.0493
T	1	-1.625022	0.77732880	-2.091	0.1717
D	1	1.624807	0.77732880	2.090	0.1718

C.5 5% Design Around 50% Step along Gradient

SAS Program:

```
option linesize=80;
data d1;
  infile 'Bdesign.dat';
  input t d y;
```

```

proc print;
proc reg;
  model y = t d;
run;

```

SAS Output:

The SAS System

16

15:55 Saturday, October 7, 1995

OBS	T	D	Y
-----	---	---	---

1	-1	-1	0.94093
2	-1	1	1.01783
3	1	-1	0.91888
4	1	1	0.94280
5	0	0	0.94190

The SAS System

17

15:55 Saturday, October 7, 1995

Model: MODEL1

Dependent Variable: Y

Analysis of Variance

Source	DF	Sum of Squares	Mean Square	F Value	Prob>F
Model	2	0.00490	0.00245	5.821	0.1466
Error	2	0.00084	0.00042		
C Total	4	0.00574			

Root MSE	0.02051	R-square	0.8534
Dep Mean	0.95247	Adj R-sq	0.7068
C.V.	2.15340		

The SAS System

18

15:55 Saturday, October 7, 1995

Parameter Estimates

Variable	DF	Parameter	Standard	T for H0:	Prob > T
		Estimate	Error	Parameter=0	
INTERCEP	1	0.952465	0.00917254	103.839	0.0001
T	1	-0.024272	0.01025521	-2.367	0.1416
D	1	0.025206	0.01025521	2.458	0.1332

C.6 5% Design on Step 9 Point

SAS Program:

```
option linesize=80;
data d1;
  infile 'Bdesign.dat';
  input t d y;
proc print;
proc reg;
  model y = t d;
run;
```

SAS Output:

The SAS System 1
15:37 Sunday, October 8, 1995

OBS	T	D	Y
1	-1	-1	0.92522
2	-1	1	0.97780
3	1	-1	0.92392
4	1	1	0.92522
5	0	0	0.92522

The SAS System 2
15:37 Sunday, October 8, 1995

Model: MODEL1

Dependent Variable: Y

Analysis of Variance

Source	DF	Sum of Squares	Mean Square	F Value	Prob>F
--------	----	----------------	-------------	---------	--------

Model	2	0.00145	0.00073	1.840	0.3521
Error	2	0.00079	0.00039		
C Total	4	0.00224			
Root MSE		0.01986	R-square	0.6479	
Dep Mean		0.93547	Adj R-sq	0.2959	
C.V.		2.12296			

The SAS System

3

15:37 Sunday, October 8, 1995

Parameter Estimates

Variable	DF	Parameter	Standard	T for H0:	
		Estimate	Error	Parameter=0	Prob > T
INTERCEP	1	0.935474	0.00888155	105.328	0.0001
T	1	-0.013471	0.00992988	-1.357	0.3077
D	1	0.013471	0.00992988	1.357	0.3077

C.7 First Ridge Analysis

SAS Program:

```
linesize=80;
data d1;
  infile='phs2.dat';
  input t d y;
proc print;
proc rsreg;
  model y = t d/nocode;
  ridge min radius = 0 to 4 by 0.1;
run;
```

SAS Output:

The SAS System

16:34 Sunday, October 8, 1995 4

OBS	T	D	Y	TD	TT	DD
1	-1.000	-1.000	0.92522	1	1.00000	1.00000
2	-1.000	1.000	0.97780	-1	1.00000	1.00000
3	1.000	-1.000	0.92392	-1	1.00000	1.00000
4	1.000	1.000	0.92522	1	1.00000	1.00000
5	0.000	0.000	0.92522	0	0.00000	0.00000
6	1.414	0.000	0.91949	0	1.99940	0.00000
7	-1.414	0.000	0.95819	0	1.99940	0.00000
8	0.000	1.414	0.95497	0	0.00000	1.99940
9	0.000	-1.414	0.91991	0	0.00000	1.99940

The SAS System 16:34 Sunday, October 8, 1995 5

Response Surface for Variable Y

Response Mean	0.936658
Root MSE	0.000898
R-Square	0.9993
Coef. of Variation	0.0959

Regression	Degrees of Freedom		Type I Sum of Squares	R-Square	F-Ratio	Prob > F
Linear	2		0.002813	0.7766	1744.2	0.0000
Quadratic	2		0.000149	0.0412	92.520	0.0020
Crossproduct	1		0.000657	0.1815	815.3	0.0001
Total Regress	5		0.003619	0.9993	897.8	0.0001

The SAS System 16:34 Sunday, October 8, 1995 6

Residual	Degrees of Freedom		Sum of Squares	Mean Square
Total Error	3		0.000002419	0.000000806

Degrees of	Parameter	Standard	T for H0:
------------	-----------	----------	-----------

Parameter	Freedom	Estimate	Error	Parameter=0	Prob > t
INTERCEPT	1	0.925218	0.000898	1030.4	0.0000
T	1	-0.013577	0.000317	-42.765	0.0000
D	1	0.012934	0.000317	40.739	0.0000
T*T	1	0.006785	0.000527	12.887	0.0010
D*T	1	-0.012819	0.000449	-28.553	0.0001
D*D	1	0.006087	0.000527	11.560	0.0014

The SAS System 16:34 Sunday, October 8, 1995 7

Factor	Degrees of Freedom		Sum of Squares	Mean Square	F-Ratio	Prob > F
T	3	0.002266	0.000755	936.7	0.0001	
D	3	0.002103	0.000701	869.5	0.0001	

The SAS System 16:34 Sunday, October 8, 1995 8

Canonical Analysis of Response Surface

Factor	Critical Value
T	-0.595868
D	-1.689911

Predicted value at stationary point 0.918335

Eigenvalues	Eigenvectors	
	T	D
0.012855	0.726087	-0.687603
0.000016930	0.687603	0.726087

Stationary point is a minimum.

The SAS System 16:34 Sunday, October 8, 1995 9

Estimated Ridge of Minimum Response for Variable Y

Radius	Estimated Response	Standard Error	Factor Values	
			T	D
0	0.925218	0.000898	0	0
0.100000	0.923471	0.000894	0.072373	-0.069009
0.200000	0.921982	0.000882	0.144656	-0.138110
0.300000	0.920750	0.000863	0.216789	-0.207371
0.400000	0.919774	0.000837	0.288631	-0.276933
0.500000	0.919056	0.000804	0.359806	-0.347188
0.600000	0.918595	0.000767	0.428764	-0.419716
0.700000	0.918390	0.000726	0.474604	-0.514540
0.800000	0.918363	0.000684	0.295297	-0.743505
0.900000	0.918355	0.000645	0.163626	-0.885001
1.000000	0.918350	0.000615	0.057195	-0.998363
1.100000	0.918346	0.000599	-0.037907	-1.099347
1.200000	0.918343	0.000604	-0.126535	-1.193310
1.300000	0.918340	0.000637	-0.210988	-1.282764
1.400000	0.918338	0.000699	-0.292543	-1.369094
1.500000	0.918336	0.000789	-0.371980	-1.453145
1.600000	0.918335	0.000904	-0.449810	-1.535471

The SAS System

16:34 Sunday, October 8, 1995 10

Radius	Estimated Response	Standard Error	Factor Values	
			T	D
1.700000	0.918335	0.001040	-0.526389	-1.616451
1.800000	0.918335	0.001196	-0.601967	-1.696359
1.900000	0.918335	0.001368	-0.676733	-1.775396
2.000000	0.918335	0.001556	-0.750829	-1.853714
2.100000	0.918337	0.001757	-0.824363	-1.931431
2.200000	0.918338	0.001971	-0.897423	-2.008639
2.300000	0.918340	0.002198	-0.970077	-2.085414
2.400000	0.918342	0.002437	-1.042383	-2.161814
2.500000	0.918344	0.002688	-1.114384	-2.237889
2.600000	0.918347	0.002950	-1.186121	-2.313681
2.700000	0.918350	0.003224	-1.257624	-2.389222
2.800000	0.918354	0.003509	-1.328920	-2.464543
2.900000	0.918358	0.003805	-1.400033	-2.539667
3.000000	0.918362	0.004112	-1.470982	-2.614615

3.100000	0.918367	0.004430	-1.541783	-2.689406
3.200000	0.918372	0.004759	-1.612451	-2.764055
3.300000	0.918377	0.005099	-1.683000	-2.838576
3.400000	0.918383	0.005449	-1.753440	-2.912979
3.500000	0.918389	0.005811	-1.823780	-2.987277
3.600000	0.918395	0.006183	-1.894030	-3.061478

The SAS System

16:34 Sunday, October 8, 1995 11

Radius	Estimated Response	Standard Error	Factor Values
			T D
3.700000	0.918402	0.006565	-1.964197 -3.135591
3.800000	0.918409	0.006959	-2.034288 -3.209622
3.900000	0.918416	0.007363	-2.104309 -3.283578
4.000000	0.918424	0.007777	-2.174265 -3.357465

C.8 Screening Design for Transport Calibration

SAS Program:

```
option linesize=80;
data d1;
  infile 'trans1.dat';
  input alphaL ratio F Rf RC y;
proc print;
proc reg;
  model y = alphaL ratio F Rf RC;
run;
```

SAS Output:

The SAS System

1

08:52 Wednesday, October 18, 1995

OBS	ALPHAL	RATIO	F	RF	RC	Y
1	-1	-1	-1	-1	-1	94.047
2	-1	-1	-1	-1	1	67.183
3	-1	-1	-1	1	-1	219.256
4	-1	-1	-1	1	1	77.893
5	-1	-1	1	-1	-1	172.274
6	-1	-1	1	-1	1	73.619

7	-1	-1	1	1	-1	273.971
8	-1	-1	1	1	1	93.629
9	-1	1	-1	-1	-1	67.183
10	-1	1	-1	-1	1	67.183
11	-1	1	-1	1	-1	67.183
12	-1	1	-1	1	1	67.183
13	-1	1	1	-1	-1	67.183
14	-1	1	1	-1	1	67.183
15	-1	1	1	1	-1	67.174
16	-1	1	1	1	1	67.183
17	1	-1	-1	-1	-1	67.183
18	1	-1	-1	-1	1	67.183
19	1	-1	-1	1	-1	78.544
20	1	-1	-1	1	1	67.183

The SAS System

2

08:52 Wednesday, October 18, 1995

OBS	ALPHAL	RATIO	F	RF	RC	Y
21	1	-1	1	-1	-1	67.051
22	1	-1	1	-1	1	67.183
23	1	-1	1	1	-1	128.365
24	1	-1	1	1	1	67.949
25	1	1	-1	-1	-1	67.183
26	1	1	-1	-1	1	67.183
27	1	1	-1	1	-1	67.183
28	1	1	-1	1	1	67.183
29	1	1	1	-1	-1	67.183
30	1	1	1	-1	1	67.183
31	1	1	1	1	-1	67.183
32	1	1	1	1	1	67.183

The SAS System

3

08:52 Wednesday, October 18, 1995

Model: MODEL1

Dependent Variable: Y

Analysis of Variance

Source	DF	Sum of Squares	Mean Square	F Value	Prob>F
--------	----	----------------	-------------	---------	--------

Model	5	31342.60698	6268.52140	4.126	0.0068
Error	26	39503.12918	1519.35112		
C Total	31	70845.73616			
Root MSE		38.97885	R-square	0.4424	
Dep Mean		86.16980	Adj R-sq	0.3352	
C.V.		45.23494			

The SAS System

4

08:52 Wednesday, October 18, 1995

Parameter Estimates

Variable	DF	Parameter	Standard	T for H0:	Prob > T
		Estimate	Error	Parameter=0	
INTERCEP	1	86.169800	6.89055314	12.505	0.0001
ALPHAL	1	-14.413200	6.89055314	-2.092	0.0464
RATIO	1	-18.987263	6.89055314	-2.756	0.0106
F	1	6.423706	6.89055314	0.932	0.3598
RF	1	10.345581	6.89055314	1.501	0.1453
RC	1	-16.214344	6.89055314	-2.353	0.0265

C.9 First-Order Design for RSM Transport Calibration

SAS Program:

```
option linesize=80;
data d1;
  infile 'trans2.dat';
  input alphaL ratio y;
  y=y-67;
proc print;
proc reg;
  model y = alphaL ratio;
run;
```

SAS Output:

The SAS System

4

17:24 Wednesday, October 18, 1995

OBS	ALPHAL	RATIO	Y
1	-1	-1	0.1906
2	-1	1	0.0921
3	1	-1	0.0505
4	1	1	0.1115

The SAS System 5
17:24 Wednesday, October 18, 1995

Model: MODEL1

Dependent Variable: Y

Analysis of Variance

Source	DF	Sum of Squares	Mean Square	F Value	Prob>F
Model	2	0.00399	0.00200	0.314	0.7838
Error	1	0.00636	0.00636		
C Total	3	0.01035			
Root MSE		0.07975	R-square	0.3857	
Dep Mean		0.11118	Adj R-sq	-0.8428	
C.V.		71.73375			

The SAS System 6
17:24 Wednesday, October 18, 1995

Parameter Estimates

Variable	DF	Parameter Estimate	Standard Error	T for H0: Parameter=0	Prob > T
INTERCEP	1	0.111175	0.03987500	2.788	0.2192
ALPHAL	1	-0.030175	0.03987500	-0.757	0.5876
RATIO	1	-0.009375	0.03987500	-0.235	0.8530

C.10 Ridge Analysis for RSM Transport Calibration

SAS Program:

```
option linesize=80;
```

```

data d1;
  infile 'trans3.dat';
  input alphaL ratio y;
proc print;
proc rsreg;
  model y = alphaL ratio/nocode;
  ridge min radius = 0 to 5 by 0.1;
run;

```

SAS Output:

The SAS System

7

17:11 Thursday, October 26, 1995

OBS	ALPHAL	RATIO	Y
1	-1.000	-1.000	67.1906
2	-1.000	1.000	67.0921
3	1.000	-1.000	67.0505
4	1.000	1.000	67.1115
5	-1.414	0.000	67.2464
6	1.000	0.000	67.0764
7	0.000	1.414	67.0327
8	0.000	-1.000	67.0394
9	0.000	0.000	67.0362

The SAS System

8

17:11 Thursday, October 26, 1995

Response Surface for Variable Y

Response Mean	67.097311
Root MSE	0.008413
R-Square	0.9953
Coef. of Variation	0.0125

Regression	Degrees		R-Square	F-Ratio	Prob > F
	of	Freedom			
Linear	2	0.018495	0.4105	130.6	0.0012

Quadratic	2	0.019983	0.4436	141.2	0.0011
Crossproduct	1	0.006360	0.1412	89.850	0.0025
Total Regress	5	0.044838	0.9953	126.7	0.0011

The SAS System

9

17:11 Thursday, October 26, 1995

Residual	Degrees of Freedom	Sum of Squares	Mean Square
Total Error	3	0.000212	0.000070786

Parameter	Degrees of Freedom	Parameter Estimate	Standard Error	T for H0: Parameter=0	Prob > T
INTERCEPT	1	67.033701	0.007201	9308.9	0.0000
ALPHAL	1	-0.033430	0.003348	-9.985	0.0021
RATIO	1	-0.006629	0.003348	-1.980	0.1421
ALPHAL*ALPHAL	1	0.079230	0.005135	15.430	0.0006
RATIO*ALPHAL	1	0.039875	0.004207	9.479	0.0025
RATIO*RATIO	1	0.000977	0.005135	0.190	0.8613

The SAS System

10

17:11 Thursday, October 26, 1995

Factor	Degrees of Freedom	Sum of Squares	Mean Square	F-Ratio	Prob > F
ALPHAL	3	0.039926	0.013309	188.0	0.0007
RATIO	3	0.006651	0.002217	31.318	0.0092

The SAS System

11

17:11 Thursday, October 26, 1995

Canonical Analysis of Response Surface

Factor	Critical Value
--------	----------------

ALPHAL	0.155432
RATIO	0.220709

Predicted value at stationary point 67.030371

Eigenvalues	Eigenvectors	
	ALPHAL	RATIO
0.084017	0.972366	0.233460
-0.003810	-0.233460	0.972366

Stationary point is a saddle point.

The SAS System

12

17:11 Thursday, October 26, 1995

Estimated Ridge of Minimum Response for Variable Y

Radius	Estimated Response	Standard Error	Factor Values	
			ALPHAL	RATIO
0	67.040977	0.007176	-0.207000	0.207000
0.100000	67.035841	0.007196	-0.110072	0.231596
0.200000	67.032385	0.007149	-0.013603	0.257968
0.300000	67.030605	0.007027	0.078622	0.298760
0.400000	67.030087	0.006669	0.068286	0.497203
0.500000	67.029660	0.006317	0.034885	0.644598
0.600000	67.029172	0.005996	0.006015	0.767914
0.700000	67.028613	0.005734	-0.020919	0.881814
0.800000	67.027981	0.005577	-0.046816	0.990799
0.900000	67.027274	0.005583	-0.072079	1.096829
1.000000	67.026492	0.005804	-0.096925	1.200923
1.100000	67.025634	0.006271	-0.121479	1.303670
1.200000	67.024701	0.006988	-0.145820	1.405439
1.300000	67.023692	0.007937	-0.170000	1.506473
1.400000	67.022607	0.009094	-0.194056	1.606940
1.500000	67.021446	0.010434	-0.218015	1.706960

The SAS System

13

17:11 Thursday, October 26, 1995

Radius	Estimated Response	Standard Error	Factor Values	
			ALPHAL	RATIO
1.600000	67.020209	0.011936	-0.241894	1.806619
1.700000	67.018897	0.013586	-0.265709	1.905986
1.800000	67.017508	0.015372	-0.289471	2.005110
1.900000	67.016043	0.017287	-0.313188	2.104030
2.000000	67.014501	0.019323	-0.336868	2.202779
2.100000	67.012884	0.021477	-0.360515	2.301381
2.200000	67.011191	0.023745	-0.384134	2.399857
2.300000	67.009421	0.026125	-0.407729	2.498224
2.400000	67.007576	0.028614	-0.431304	2.596495
2.500000	67.005654	0.031212	-0.454860	2.694683
2.600000	67.003656	0.033916	-0.478399	2.792796
2.700000	67.001582	0.036727	-0.501924	2.890844
2.800000	66.999431	0.039643	-0.525436	2.988834
2.900000	66.997205	0.042664	-0.548937	3.086771
3.000000	66.994902	0.045790	-0.572427	3.184661
3.100000	66.992523	0.049019	-0.595908	3.282508
3.200000	66.990068	0.052351	-0.619380	3.380317
3.300000	66.987537	0.055787	-0.642845	3.478091
3.400000	66.984929	0.059326	-0.666303	3.575834

The SAS System

14

17:11 Thursday, October 26, 1995

Radius	Estimated Response	Standard Error	Factor Values	
			ALPHAL	RATIO
3.500000	66.982246	0.062968	-0.689754	3.673547
3.600000	66.979486	0.066712	-0.713200	3.771234
3.700000	66.976650	0.070559	-0.736640	3.868896
3.800000	66.973738	0.074508	-0.760075	3.966536
3.900000	66.970750	0.078559	-0.783505	4.064155
4.000000	66.967685	0.082713	-0.806931	4.161754
4.100000	66.964544	0.086968	-0.830354	4.259336
4.200000	66.961327	0.091326	-0.853772	4.356902
4.300000	66.958034	0.095785	-0.877188	4.454452
4.400000	66.954665	0.100346	-0.900600	4.551988
4.500000	66.951219	0.105009	-0.924009	4.649510
4.600000	66.947698	0.109774	-0.947415	4.747020

4.700000	66.944100	0.114641	-0.970819	4.844519
4.800000	66.940425	0.119609	-0.994221	4.942006
4.900000	66.936675	0.124679	-1.017620	5.039483
5.000000	66.932849	0.129851	-1.041017	5.136951

Appendix D. FORTRAN

D.1 Root Mean Squared Error Criterion Program

```
program eval
*****
*      this program evaluates the RMS error criterion from
*      a given run of Bioplume.  It reads the actual
*      final contaminant concentrations and heads from the files
*      water991.final and snap5.final and compares the values
*      to the predicted final values in the files heads.pre
*      and conc.pre.  Note that i=column(1-20) and j=row (1-30)
*****
integer i,j,junk
real predhead(30,20),predbenz(30,20),actthead(30,20),
1 actbenz(30,20),sumheads,sumtrans
open(unit=1,file='wtrfinal.bio',status='old',access=
1 'sequential',form='formatted')
open(unit=2,file='snap5.bio',status='old',access=
1 'sequential',form='formatted')
open(unit=3,file='HEADS.BIO',access='sequential',
1 form='formatted')
open(unit=4,file='HPLUME.BIO',access='sequential',
1 form='formatted')
sumheads=0
sumtrans=0
junk=0
*****
*      Fill the arrays up with zeros
*****
do 100 i=1,20
  do 200 j=1,30
    predhead(j,i)=0.0
    predbenz(j,i)=0.0
    actthead(j,i)=0.0
    actbenz(j,i)=0.0
200  continue
100  continue
*****
*      Read the actual heads and concentrations into arrays
*****
300  do 400 j=1,30
      read (1,*) (actthead(j,i),i=1,20)
```

```

        read (2,*) (actbenz(j,i),i=1,20)
400  continue
*****
*      Read the predicted heads and concentrations into arrays
*****
500  do 550 j=1,30
      read (unit=3,fmt=*,err=600) (predhead(j,i),i=1,20)
550  continue
      goto 500
600  continue
      read (unit=4,fmt=*,err=675) junk
      do 650 j=1,30
          read (4,*) (predbenz(j,i),i=1,20)
650  continue
      goto 600
*****
*      Calculate the RMS error criterion and print results
*****
675  do 700 i=1,20
      do 800 j=1,30
          sumheads=sumheads+(acthead(j,i)-predhead(j,i))**2
          sumtrans=sumtrans+(actbenz(j,i)-predbenz(j,i))**2
800  continue
700  continue
      RMSflow=(sumheads/600)**0.5
      RMStrans=(sumtrans/600)**0.5
*      print *, 'print out the predbenz array (should be all zeros):'
*      print *, predbenz
*      print *, 'print out the actbenz array:'
*      do 1000 i=1,20
*          do 2000 j=1,30
*              print *, 'actbenz(row=',j,',col=',i,')=',actbenz(j,i)
2000  continue
1000 continue
*      print *, 'sumheads=',sumheads
*      print *, 'sumtrans=',sumtrans
*      do 3000 j=1,30
*          do 3100 i=1,20
*              print *, acthead(j,i), ' vs ', predhead(j,i)
3100  continue
3000 continue
*      do 4000 j=1,30

```

```
*      do 4100 i=1,20
*      print *,actbenz(j,i), ' vs ',predbenz(j,i)
4100  continue
4000  continue
      print *, 'RMSflow=' , RMSflow
      print *, 'RMStrans=' , RMStrans
      print *, 'done'
      end
```

Bibliography

1. Adams, Leo C. *Estimating groundwater flow parameters using response surface methodology*. AFIT/GSO/ENS/94A-01, School of Engineering, Air Force Institute of Technology (AU), Wright-Patterson Air Force Base, 1994.
2. Anderson, Mary P. and William W. Woessner. *Applied Groundwater Modeling, Simulation of Flow and Advective Transport*. San Diego, CA: Academic Press, Inc., 1992.
3. Angley, Joseph T. and others. "Nonequilibrium Sorption and Aerobic Biodegradation of Dissolved Alkylbenzenes during Transport in Aquifer Material: Column Experiments and Evaluation of a Coupled Process Model," *Environmental Science and Technology*, 26:1404–1410 (July 1992).
4. Atlas, Ronald M. and Richard Bartha. *Microbial Ecology, Fundamentals and Applications* (3rd Edition). Redwood City, California: The Benjamin Cummings Publishing Co., Inc., 1993.
5. Auclair, Paul F. "RSM Class Notes." Unpublished notes from class at Air Force Institute of Technology, July 1995.
6. Baedecker, Mary Jo and others. "Crude Oil in a shallow sand and gravel aquifer - III. Biogeochemical reactions and mass balance modeling in anoxic groundwater," *Applied Geochemistry*, 8:569–586 (1993).
7. Bair, Scott E. and others. "Particle-Tracking Analysis of Flow Paths and traveltimes from Hypothetical Spill Sites Within the Capture Area of a Wellfield," *Ground Water*, 28:884–892 (November-December 1990).
8. Bak, F. and F. Widel. "Anaerobic degradation of phenol and phenol derivatives by *Desulfovobacterium phenicolum* sp. nov.," *Archives of Microbiology*, 146:177–180 (1986).
9. Boggs, J. M. and others. *Database for the Second Macrodispersion Experiment (MADE-2)*. Interim Report EPRI TR-102072, Norris, Tennessee: Tennessee Valley Authority, February 1993.
10. Boggs, J. Mark and others. "Field Study of Dispersion in a Heterogeneous Aquifer, 1. Overview and Site Description," *Water Resources Research*, 28(12):3281–3291 (December 1992).
11. Borden, Robert C. "Natural Bioremediation of Hydrocarbon-Contaminated Ground Water." *Handbook of Bioremediation* edited by John E. Mathews, Boca Raton: Lewis Publishers, 1994.
12. Box, George P. and Norman R. Draper. *Empirical Model Building and Response Surfaces*. Wiley Series in Probability and Mathematical Statistics, New York: John Wiley and Sons, 1987.
13. Brooks, Roger J. and others. "Determining the range of predictions of a groundwater model which arises from alternative calibrations," *Water Resources Research*, 30:2993–3000 (November 1994).

14. Butcher, Jonathan B. and Thomas D. Gauthier. "Estimation of Residual NAPL Mass by Inverse Modeling," *Ground Water*, 32:71–78 (January–February 1994).
15. Carrera, J. and L. Glosorio. "On geostatistical formulations of the groundwater flow inverse problem," *Advances in Water Resources*, 14:273–283 (1991).
16. Carrera, Jesus and Schlomo P. Neuman. "Estimation of Aquifer Parameters Under Transient and Steady State Conditions: 1. Maximum Likelihood Method Incorporating Prior Information," *Water Resources Research*, 22:199–210 (February 1986a).
17. Carrera, Jesus and Schlomo P. Neuman. "Estimation of Aquifer Parameters Under Transient and Steady State Conditions: 2. Uniqueness, Stability, and Solution Algorithms," *Water Resources Research*, 22:211–227 (February 1986b).
18. Chapelle, Francis H. *Ground-Water Microbiology and Geochemistry*. New York: John Wiley and Sons, 1993.
19. Cottman, Richard M. *Groundwater Model Parameter Estimation Using Response Surface Methodology*. AFIT/GOR/ENS/95M, School of Engineering, Air Force Institute of Technology (AU), Wright-Patterson Air Force Base, March 1995.
20. Cozzarelli, Isabelle M. and others. "Transformation of Monoaromatic Hydrocarbons to Organic Acids in Anoxic Groundwater Environment," *Environmental Geology and Water Science*, 16:135–141 (1990).
21. Cozzarelli, Isabelle M. and others. "The geochemical evolution of low-molecular-weight organic acids derived from the degradation of petroleum contaminants in groundwater," *Geochemica et Cosmochimica*, 58:863–877 (1994).
22. Cutright, Teresa J. and Sunggyu Lee. "In-Situ Bioremediation of PAH Contaminated Soil Using *Mycobacterium* sp.," *Fresenius Environmental Bulletin*, 3:400–406 (July 1994).
23. Davis, John W. and others. "Natural Biological Attenuation of Benzene in Ground Water Beneath a Manufacturing Facility," *Ground Water*, 32:215–226 (March–April 1994).
24. de Marsily, Ghislain. *Quantitative Hydrogeology, Groundwater Hydrology for Engineers*. Orlando, Florida: Academic Press Inc., 1986. Translated by Gunilla de Marsily.
25. Devlin, J. F. "A Simple and Powerful Method of Parameter Estimation Using Simplex Optimization," *Ground Water*, 32:323–327 (March–April 1994).
26. Doughty, Christine and others. "Hydrologic characterization of heterogeneous geologic media with an inverse method based on iterated function systems," *Water Resources Research*, 30:1721–1745 (June 1994).
27. Freeze, R. Allen and others. "Hydrogeologic decision Analysis: 1. A Framework," *Ground Water*, 28:738–766 (September–October 1990).
28. Grbic-Galic, D. and T. M. Vogel. "Transformation of toluene and benzene by mixed methanogenic cultures," *Applied and Environmental Microbiology*, 53:254–260 (1987).

29. Heitkamp, M. A. and C. E. Cerniglia. "Mineralization of polycyclic aromatic hydrocarbons by a bacterium isolated from sediment below an oil field," *Environmental Microbiology*, 54:1612–1614 (1988).
30. Hund, Kerstin and Birgit Schenk. "The Microbial Respiration Quotient as indicator for the bioremediation process," *Chemosphere*, 28:477–490 (February 1994).
31. Keckler, Doug. *Surfer for Windows User's Guide, Contouring and 3D Surface Mapping*. Golden Software, Inc., Golden, Colorado, February 1994.
32. Keidser, Allan and Dan Rosbjerg. "A Comparison of Four Inverse Approaches to Groundwater Flow and Transport Parameter Identification," *Water Resources Research*, 27:2219–2232 (September 1991).
33. Kerfoot, H. B. "In Situ Determination of the Rate of Unassisted Degradation of Saturated-Zone Hydrocarbon Contamination," *Journal of the Air and Waste Management Association*, 44:877–880 (July 1994).
34. Konikow, L. F. and J. D. Bredehoeft. "Techniques of Water Resources Investigations of the United States Geological Survey." *Computer Model of Two-Dimensional Solute Transport and Dispersion in Ground Water*, (2nd Edition) Automated Data Processing and Computations, chapter C2, United States Geological Survey, 1984.
35. Leahy, J. G. and R. R. Colwell. "Microbial degradation of hydrocarbons in the environment," *Microbiological Reviews*, 54:305–315 (1990).
36. Liss, Steven N. and Katherine H. Baker. "Anoxic/Anaerobic Bioremediation." *Bioremediation* edited by Katherine H. Baker and Diane S. Herson, New York: McGraw-Hill, 1994.
37. Madsen, Eugene L. and others. "In Situ Biodegradation: Microbiological Patterns in a Contaminated Aquifer," *Science*, 252:830–833 (May 1991).
38. McAllister, P. M. and C. Y. Chiang. "A Practical Approach to Evaluating Natural Attenuation of Contaminants in Ground Water," *Ground Water Monitoring and Remediation*, 161–173 (Spring 1994).
39. Mercado, Abraham. "A Note on Micro and Macrodispersion," *Ground Water*, 22(6):790–791 (Nov-Dec 1984).
40. Morgan, Philip and others. "Biodegradation of Benzene, Toluene, Ethylbenzene, and Xylenes in Gas-Condensate-Contaminated Ground-Water," *Environmental Pollution*, 82:181–190 (1993).
41. Nielsen, Per H. and others. "A Field Method for Determination of groundwater Sediment Associated Potentials for Degradation of Xenobiotic Compounds," *Chemosphere*, 25:449–462 (1992).
42. Olsthoorn, T. N. "Effective Parameter Optimization for Ground-Water Model Calibration," *Ground Water*, 33:42–48 (January-February 1995).

43. Rainwater, Ken and Richard J. Scholze. "In-Situ Biodegradation of Contaminated Soil and Groundwater." *Biological Processes 3. Innovative Hazardous Waste Treatment Technology*, edited by Harry M. Freeman and P. R. Sferra, Cincinnati, Ohio: Risk Reduction Engineering Laboratory, 1991.
44. Richter, J. and others. "Use of combinations of lumped parameter models to interpret groundwater isotopic data," *Journal of Contaminant Hydrology*, 14:1-13 (1993).
45. Rifai, Hanadi, "Telephone Conversation with Dr. Hanadi Rifai regarding Bioplume," June 1995.
46. Rifai, Hanadi and others. *Bioplume II Computer Model of Two-Dimensional Contaminant Transport Under the Influence of Oxygen Limited Biodegradation in Ground Water*. National Center for Ground Water Research, Rice University, Houston, Texas, October 1987.
47. Rifai, Hanadi S. and others. "Biodegradation Modeling at Aviation Fuel Spill Site," *Journal of Environmental Engineering*, 114:1007-1029 (October 1988).
48. Rifai, Hanadi S. and others. "Simulation of Natural Attenuation with Multiple Electron Acceptors." *Intrinsic Bioremediation 1. Proceedings of Third International In Situ and On-Site Bioreclamation Symposium*, edited by Robert E. Hinchee, et al. 53-58. Columbus: Battelle Press, April 1995.
49. Spear, Robert C. and others. "Parameter uncertainty and interaction in complex environmental models," *Water Resources Research*, 30:3159-3169 (November 1994).
50. Stauffer, Thomas B. and others. *Degradation of Aromatic Hydrocarbons in an Aquifer During a Field Experiment Demonstrating the Feasibility of Remediation by Natural Attenuation*. Final Technical report for Period October 1989 - September 1992 AL/EQ-TR-1993-0007, Tyndall Air Force Base, Florida: Armstrong Laboratory, Department of the Air Force, April 1994.
51. Stauffer, Thomas B. and others. "A Natural Gradient Tracer Experiment in a Heterogeneous Aquifer With Measured In-Situ Biodegradation Rates: A Case for Natural Attenuation." *Symposium on Intrinsic Bioremediation of Ground Water*. 73-84. 1994.
52. Sun, Ne-Zheng and others. "A proposed geological parameterization method for parameter identification in three-dimensional groundwater modeling," *Water Resources Research*, 31:89-102 (January 1995).
53. Szewzyk, R. and N. Pfennig. "Complete oxidation of catechol by strictly anaerobic sulfate reducing *Desulfovobacterium catecholicum* sp. nov.," *Archives of Microbiology*, 147:163-168 (1987).
54. Trower, M. K. and others. "Isolation and characterization of a cyclohexane-metabolizing *Xanthobacter* sp.," *Applied and Environmental Microbiology*, 49:1282-1289 (1985).
55. Vogel, T. M. and D. Grbic-Galic. "Incorporation of oxygen from water into toluene and benzene during anaerobic fermentative transformation," *Applied and Environmental Microbiology*, 52:200-202 (1986).

56. Walton, William C. *Principles of Groundwater Engineering*. Chelsea, Michigan: Lewis Publishers, 1991.
57. Willis, Robert and William W-G. Yeh. *Groundwater Systems Planning and Management*. Englewood Cliffs, New Jersey: Prentice-Hall, 1987.
58. Wilson, Barbara H. and others. "Biotransformations of Selected Alkylbenzenes and Halogenated Aliphatic Hydrocarbons in Methanogenic Aquifer Material: A Microcosm Study," *Environmental Science and Technology*, 20:997-1002 (1986).
59. Wilson, John T. and others. "Intrinsic bioremediation of JP-4 Jet Fuel." *Symposium on Intrinsic Bioremediation of Ground Water*. 60-72. 1994.
60. Wise, William R. and Randall J. Charbeneau. "In-Situ Estimation of Transport Parameters: A Field Demonstration," *Ground Water*, 32:420-430 (May-June 1994).
61. Wood, W. L. *Introduction to Numerical Methods for Water Resources*. Oxford Science Publications, Oxford: Clarendon Press, 1993.
62. Yeh, T.C. Jim and others. "An Iterative Cokriging-Like Technique for Ground-Water Flow Modeling," *Ground Water*, 33:33-41 (January-February 1995).
63. Yeh, William W-G. "Review of Parameter Identification Procedures in Groundwater Hydrology: The Inverse Problem," *Water Resources Research*, 22:95-108 (February 1986).
64. Young, Steven C. and J. Mark Boggs. "Observed Migration of a Tracer Plume at the MADE Site." *Proceedings: Environmental Research Conference on Groundwater Quality and Waste Disposal*, number EN-6749, edited by I. P. Murarka and S. Cordle. 11-1 to 11-22. Palo Alto, California: Electric Power Research Institute, March 1990.
65. Zeyer, J. and others. "Rapid microbial mineralization of toluene and 1,3-dimethylbenzene in the absence of molecular oxygen," *Applied and Environmental Microbiology*, 52:944-947 (1986).

Vita

Benjamin Shuman was born [REDACTED] November 7, 1966 in [REDACTED] [REDACTED]. He graduated from the George Washington Carver High School of Engineering and Science in 1986. In January 1989, after moving to Eureka, California, he married Lori L. Williams. In [REDACTED] he earned his Engineer-In-Training Certificate from the State of California. In May of 1993 he graduated from Humboldt State University, in Eureka, with a Bachelor of Science Degree in Environmental Resources Engineering. Immediately following graduation he reported to Scott AFB, Illinois. At Scott AFB he worked as a PALACE Acquire Intern in the Environmental Division of Headquarters Air Mobility Command's Civil Engineering Directorate, completing an extensive training program, overseeing program funding for Environmental Compliance at two AMC bases and managing the command's Lead Based Paint Program. His son Aaron was born [REDACTED]. In June 1994 he entered the School of Engineering at the Air Force Institute of Technology. Ben and Lori's second child, Emilia was born [REDACTED]. They will PCS to Pope AFB in January where Ben will work in the Analysis section of the Environmental flight.

Permanent address: 1501 Keystone Ave.
Upper Darby, PA 19082